Characterization and Modeling of Marine Channels for Millimeter Radiowaves

A thesis submitted to the
Graduate School of Natural and Applied Sciences

by

Niloofar Mehrnia

in partial fulfillment for the
degree of Master of Science

in

Electronics and Computer Engineering

This is to certify that we have read this thesis and that in our opinion it is fully adequate, in scope and quality, as a thesis for the degree of Master of Science in Electronics and Computer Engineering.

APPROVED BY:

Assist. Prof. Dr. Mehmet Kemal Özdemir (Thesis Advisor) .....

Assist. Prof. Dr. Hakan Doğan .....

Assist. Prof. Dr. Tunçer Baykaş .....

This is to confirm that this thesis complies with all the standards set by the Graduate School of Natural and Applied Sciences of İstanbul Şehir University:

DATE OF APPROVAL: May 2017

SEAL/SIGNATURE:

Declaration of Authorship

I, Niloofar Mehrnia, declare that this thesis titled, 'Characterization and Modeling of Marine Channels for Millimeter Radiowaves' and the work presented in it are my own. I confirm that:

- This work was done wholly or mainly while in candidature for a research degree at this University.
- Where any part of this thesis has previously been submitted for a degree or any other qualification at this University or any other institution, this has been clearly stated.
- Where I have consulted the published work of others, this is always clearly attributed.
- Where I have quoted from the work of others, the source is always given. With the exception of such quotations, this thesis is entirely my own work.
- I have acknowledged all main sources of help.
- Where the thesis is based on work done by myself jointly with others, I have made clear exactly what was done by others and what I have contributed myself.

Signed: 

Date: 22.05.2017

Characterization and Modeling of Marine Channels for Millimeter Radiowaves

Niloofar Mehrnia

Abstract

In this work, we present and analyze the simulation results of millimeter-wave propagation channel performed over the sea surface for off shore ship to ship scenario. We present a channel characterization study where channel parameters such as path loss, received power, root mean square delay spread, and power delay profile are inspected by taking the ray tracing advantages of the "Wireless InSite" software. 35 GHz and 94 GHz are the bands of interest, as they have minimum water and oxygen attenuation and their performances in practice would be the best among the other frequency bands. In our study, we investigate the effect of ray spacing, Earth's curvature, and the sea surface roughness on marine channel characteristics. Our results demonstrate that 2-ray analytical model should be only used for some short ranges over the sea surface propagating at high frequencies. Besides, free space path loss model cannot predict the behavior of channel over the sea surface in high frequencies even for the short ranges. Moreover, the main time dispersion parameters of maritime channel such as mean excess delay, Root Mean Square (RMS) delay spread, coherence bandwidth (B_c), Doppler spread as well as coherence time and coherence distance have been investigated in this work. Cumulative Distribution Functions (CDFs) of time delay parameters indicate that the maritime channels can be assumed frequency non-selective as long as the bandwidth of transmitted signal does not exceed 750 MHz and 1.53 GHz at 35 GHz and 94 GHz, respectively. In addition, based on the results obtained from the Doppler spectrum, the sea channel is not affected by vessel movements and therefore the efficacy of Doppler frequency is negligible in maritime environments at these two frequencies. Consequently, the corresponding coherence times are relatively long enough not to cause distortion due to motion. As for the coherence distance, our results illustrate that the coherence distance for off shore marine channels is so large that it offers no space diversity over the sea channel. Therefore, this thesis study is prior in considering both large and small scale variations for two different frequencies at the range of millimeter radiowave.

Keywords: Channel modeling, ray tracing, maritime channel, millimeter radiowaves, mean excess delay, RMS delay spread, coherence bandwidth, coherence distance, Doppler spread

Milimetre Radyo Dalgaları için Deniz Kanallarının Karakterizasyon ve Modellemesi

Niloofar Mehrnia

Öz

Bu çalışmada, deniz kanallarında denize açılmış gemiden gemiye milimetre dalga yayılım simülasyon sonuçları verilmiş ve analiz edilmiştir. "Wireless InSite" yazılımının ışın izleme avantajı kullanılarak, kanalın yol kaybı, alınan güç, ortalama karekök (RMS) gecikme yayılımı ve güç gecikme profili gibi kanal parametreleri dikkate alınarak kanal karakterizasyonu yapılmıştır. Minimum su ve oksijen zayıflamasına sahip olan 35 GHz ve 94 GHz pratikteki performanslarıyla diğer bantlara kıyasla daha iyi sonuç vermesi dolayısıyla seçilmiş bantlardır. Çalışmamızda ışın aralığının, yeryüzü eğriliğinin ve denizin yüzey pürüzlülüğünün deniz kanallarının özelliklerine etkisi araştırılmıştır. Elde ettiğimiz sonuçlar 2-ışını (2-ray) analitik modelinin sadece yüksek frekanslarda yayılım gösteren deniz üzerinde kısa menzillerde kullanılması gerektiğini göstermektedir. Bunların dışında serbest uzay yolu kaybı modeli kanalların su yüzeyindeki davranışlarını yüksek frekansta kısa mesafede olsa bile görememektedir. Ayrıca bu çalışmada deniz aşırı kanalların ortalama kanal gecikmesi, ortalama karekök (RMS) gecikme yayılımı, uyumluluk bant genişliği, Doppler yayılımı ve uyumluluk zamanı ve mesafesi de analiz edilmiştir. Zaman gecikme parametrelerinin Kümülatif Dağılım Fonksiyonları (CDFs) 35 GHz ve 94 GHz de gönderilen sinyallerin bant genişlikleri 750 MHz ve 1.53 GHz'i aşmadığı sürece deniz kanallarının frekans seçici olmadığı kabul edilebileceğini göstermektedir. Bunlara ek olarak, Doppler spektrumundan elde edilen sonuçlara göre deniz kanalları gemilerin hareketinden etkilenmez ve bu nedenle bu iki frekansta deniz ortamında Doppler frekansının etkisi ihmal edilebilir. Sonuç olarak, karşılık gelen uyumluluk süresi hareketten dolayı distorsiyon meydana getirmeyecek kadar uzundur. Uyumluluk mesafesine gelince, sonuçlarımız denize açılmış gemiler için deniz kanallarının uyumluluk mesafesinin çok büyük olmasından ötürü deniz kanallarında bir çeşitlilik sunmamaktadır. Dolayısıyla, bu tez çalışması milimetre dalga aralığındaki iki frekans için hem büyük hem de küçük ölçekli varyasyonları değerlendirdiği için önemlidir.

Anahtar Sözcükler: Kanal modelleme, ışın takibi, deniz kanalı, milimetre radyo dalgaları, ortalama kanal gecikmesi, RMS gecikme yayılımı, uyumluluk bant genişliği, uyumluluk mesafesi, doppler yayılımı

Acknowledgments

Indeed words are powerless to express my most valuable gratitude to my advisor Asst. Prof. Mehmet Kemal Özdemir for his support, motivation, patience, and immense knowledge. I can't imagine having a better advisor for my M.Sc. study.

Beside my advisor, I would like to appreciate the rest of my thesis committee, Asst. Prof. Hakan Doğan and Asst. Prof. Tunçer Baykaş for their insightful comments.

Last but not the least, I wish to thank my family, who are not with me but their prays always accompany me, and my good friends for their encouragement throughout my life and study.

Contents

List of Figures

List of Tables

Abbreviations

G	**G**eneration
AMPS	**A**dvance **M**obile **P**hone **S**ystems
FDMA	**F**requency **D**evision **M**ultiple **A**ccess
CDMA	**C**ode **D**evision **M**ultiple **A**ccess
UMTS	**U**niversal **M**obile **T**elecommunications **S**ystem
EDGE	**E**nhanced **D**ata for **G**SM **E**volution
OFDM	**O**rtogonal **F**requency **D**ivision **M**ultiplexing
MIMO	**M**ultiple **I**nput **M**ultiple **O**utput
WWWW	**W**orld **W**ide **W**eb **W**orm
TDMA	**T**ime **D**ivision **M**ultiple **A**ccess
PSTN	**P**ublic **S**witched **T**elephone **N**etwork
ToA	**T**ime **o**f **A**rrival
AoA	**A**ngle **o**f **A**rrival
PDP	**P**ower **D**elay **P**rofile
RMS	**R**oot **M**ean **S**quare
UTD	**U**niform **T**heory of **D**iffraction
FDTD	**F**inite **D**istance **T**ime **D**omain
NLoS	**N**on-**L**ine **o**f **S**ight
LoS	**L**ine **o**f **S**ight
USV	**U**nmanned **S**urface **V**ehicle
FFT	**F**ast **F**ourier **T**ransform
IFFT	**I**nverse **F**ast **F**ourier **T**ransform
FSL	**F**ree **S**pace Path **L**oss
TX	**T**ransmitter
RX	**R**eceiver

SBR	**S**hooting and **B**ouncing **R**ays
RMSE	**R**oot **M**ean **S**quare **E**rror
VHF	**V**ery **H**igh **F**requency
UHF	**U**ltra **H**igh **F**requency
GO	**G**eometric **O**ptics
CDF	**C**umulative **D**istribution **F**unction

Chapter 1

Introduction

There are some strong evidences that shows the wireless and mobile communications are developing so fast; evidences such as remarkable improvements in fields of mobile applications and services, wireless access networks, and subscribes [5]. In the last decades, significant changes occurred in the area of Mobile Wireless Communication networks. The mobile wireless Generation (G) refers to an either slight or considerable change in essence of the system, frequency, available bandwidth, speed, latency, an so on. Each generation has its own features which make it different from the previous generations [6].

The first generation (1G) mobile communication was used only for voice calls based on the frequency modulated analog systems. This Advanced Mobile Phone System (AMPS) applied Frequency Division Multiple Access (FDMA) with 30kHz channel bandwidth [7]. The second generation (2G) is a digital technology and supports text messaging beside voice call technology. 2G overcame some of the weaknesses of first generation by increasing the privacy, better coverage and capacity [8]. The third generation (3G) mobile technology provided higher transmission data rate, more capacity and multimedia support. The fourth generation (4G) has all advantages of 3G as well as fixed internet to emerge wireless mobile internet, which is an evolution to mobile technology and it overcame the limitations of 3G. It also reduces the resources cost and increases the available bandwidth. Figure 1.1 categorizes different communications technologies into 1G to 4G [1].

5G stands for 5th Generation Mobile technology and it will be a new revolution in mobile market which allows the cell phones to use very high bandwidth. It will be

TABLE 1.1: Comparison of all generations of mobile technologies [4]

Technology	1G	2G	3G	4G	5G
Start/ Deployment	1970-1980	1990-2004	2004-2010	Now	Soon (probably 2020
Data Bandwidth	2kbps	64kbps	2Mbps	1 Gbps	Higher than 1Gbps
Technology	Analog cellular technology	Digital cellular technology	CDMA 2000, Bluetooth, UMTS, EDGE)	Wi-Max, LTE, Wi-Fi, OFDM, MIMO	WWWW (comming soon)
Service	Mobile telephony (voice)	Digital voice, SMS, Higher capacity, Packetized data	Integrated high quality audio, video and data	Dynamic information access, Wearable devices	Dynamic information acess, Wearable devices with all capabilities
Multi -plexing	FDMA	TDMA, CDMA	CDMA	CDMA	CDMA
Switching	Circuit	Circuit, Packet	Packet	All packet	All packet
Core Network	PSTN	PSTN	Packet N/W	Internet	Internet

the first time that users experience such powerful technology, which includes all types of advance features. Therefore, it is expected that 5G technology will be the most demanded ecosystem in the close future [8].

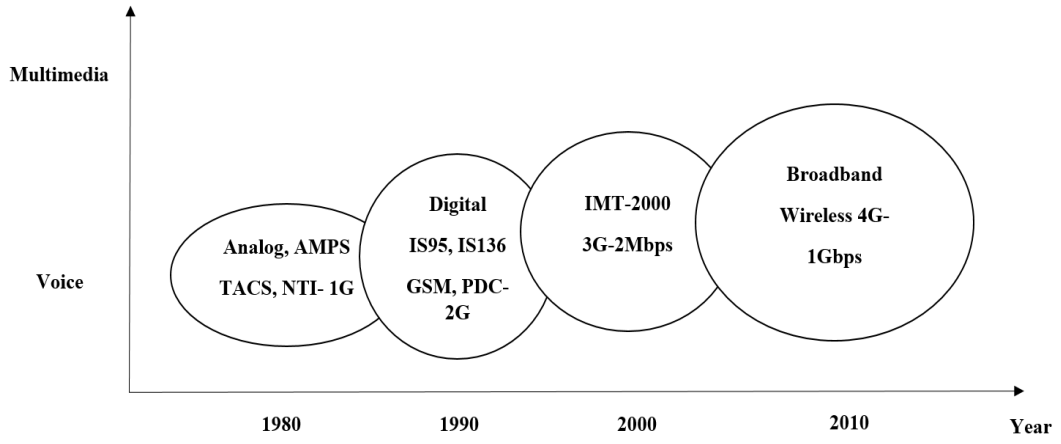

FIGURE 1.1: Evolution of communication networks [1].

The most important subjects in 5G vision is the spectrum issue. From many countries, Governments, agencies, standardization organizations and research institutions pay great

attention to the strategies of 5G spectrum [9]. Expected 5G networks will use millimeter wave band which are suitable for high data throughput in indoor scenarios, where the propagation losses are sufficiently small and the channels are basically line-of-sight. [10] presents an inclusive study in analyzing and simulating the performance of 5G- Millimeter radiowaves specially for outdoor propagation.

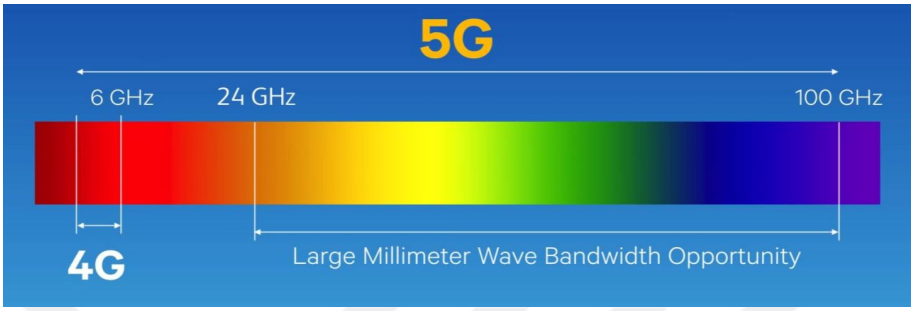

FIGURE 1.2: 5G expected spectrum [2].

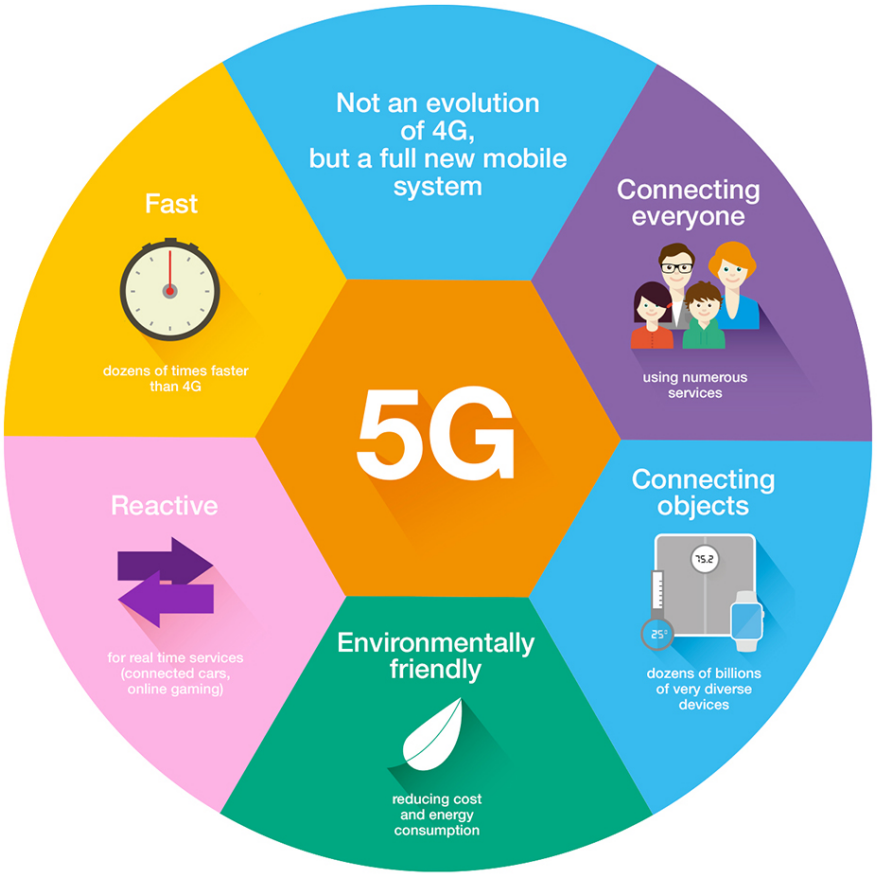

FIGURE 1.3: Features of 5G [3].

1.1 Motivation and Contribution

Although the propagation characteristics for millimeter waves in indoor and urban areas have been investigated in the last decades, amount of studies on marine environments is very low. In addition, among all studies done over the sea surface, only a few of them have focused on millimeter radiowaves [11]-[13].

In this thesis, we introduce a new maritime channel modeling approach to investigate channel characteristics over the sea. Our study is based on "Wireless InSite" tool. Although the main usage of this tool is to analyze the radio propagation for indoor and urban areas, we take advantage of the ray tracing features of this software that allows an accurate description for the interaction of rays within a maritime environment.

In "Wireless InSite" we are able to create the simulation environment and then specify its geometry, the terrain's material and dimension, location and height of transceivers, antenna type and frequency as well as the waveform and bandwidth. In order to define the maritime environment, we need to specify permittivity and conductivity of sea water as the terrain material properties. Once the simulation begins to run, a number of transmission, reflection, and diffraction happens between the transmitter-receiver and other objects in the simulation environment. These interactions help us to better understand the channel behavior within the emulated environment.

Through our problem framework setup, we compute some channel properties such as propagation loss, time of arrival (ToA), and angle of arrival (AoA) for two different frequency bands of 35 GHz and 94 GHz. After that, they all get imported to Matlab® and processed to predict other channel parameters like received power, power delay profile (PDP), root mean square (RMS) delay spread, etc.

"Wireless InSite 2.6.3" is a powerful electromagnetic modeling tool that predicts the terrain and building effects on the propagation of electromagnetic waves and then computes the characteristics of propagated signal [14]. The tool accomplishes these by shooting rays from a transmitter, and then propagating the rays through a defined environment. The rays moving toward the receiver have numerous interactions with the features. These Interactions include transmission through features, reflections from the feature faces, and diffraction around objects.

Various ray-based propagation models such as Full 3D, Vertical Plane, and Urban Canyon have been provided by Wireless InSite software. These models integrate ray tracing algorithms with the Uniform Theory of Diffraction (UTD). The propagated paths are detected by ray tracing method while the relevant complex electric field should be evaluated by UTD.

In addition to the ray-based methods, Wireless InSite provides several additional models: Free Space, Empirical Hata, and Cost-Hata. A full-wave Urban Canyon FDTD model and Moving Window FDTD model are also available.

Since this study is ray tracing based and we consider only transmitter and receiver on our terrain, Full 3D and Vertical Plane will be applied in our simulations. These tow models will be discussed in detail later in Chapter 3 and Chapter 4.

The outline for the rest of the thesis is as follows: Chapter 2 will give a brief overview over the marine channel modeling. Chapter 3 will express the large scale variations and the effect of different parameters on maritime channel. Chapter 4 then discusses the small scale behavior of channel over the sea surface with considering all parameters discussed in Chapter 3. Finally Chapter 5 concludes the work and predicts the future work.

Chapter 2

Literature Review

The previous chapter includes the introduction and motivation of our work. It discussed the improvements from 1G to 5G and the significance of millimeter radiowaves channel modelling. In addition, a brief introduction on the applied software, Wireless Insite, was given. In this chapter, we will overview the studies which focus on maritime channel modeling.

2.1 Literature Review on Large and Small Scale Variations

Over the years, radiowave propagation for marine environment has evoked interest from researchers for different communication scenarios and frequencies [15]- [27]. While some studies focus on the evaporation duct height effect in marine environment [21], [23], others deal with the impact of different frequencies or different parameters such as antenna height over the sea channels [17], [20], [25]-[26]. In spite of growing literature on channel modeling in marine environments, there is a lack of proper channel modeling approach for millimeter radiowave especially when the requirements of the new cellular systems such as 5G are discussed. In most of the studies done over maritime environments, 5 GHz frequency band have been considered since they are generally available and free for everyone to use.

As an example, [16] presented experimental propagation measurements over the sea at 5.8 GHz for a wireless communication link between two antenna, one installed at a boat and another one installed onshore. Although the study focuses on non line-of-sight (NLoS)

measurements, it has been found that 2-ray model can be fitted to the measured path loss reasonably well when Line-of-Sight (LoS) condition exists. However, with the existence of several obstacles such as ships, the received signal had been observed to attenuate more and therefore a multi-slope path loss model was proposed.

Same as [16], the authors in [18] demonstrated that at short distances the attenuation rate of transmitted signal is so close to the rate of attenuation of 2-ray model. However, when the distance is very large, although the LoS condition is preserved, the received signal attenuates at a higher rate when compared to 2-ray analytical model.

An investigation of LoS radiowave propagation at 5 GHz was presented in [19]. This work also confirmed that there is good agreement between the experimental results with the predicted values using . However, with the increase of distance, 2-ray model loses its ability to predict the propagation loss due to the existence of evaporation duct height over the sea surface. Then, 3-ray path loss model is introduced that takes into consideration both the reflected path from the sea surface and the refracted one caused by evaporation duct layer. However, this work has not shown the accuracy of their model for the higher frequencies such as millimetre waves.

[25] and [26] investigated the NLoS maritime mobile radio channels at 5 GHz. They have considered several types of cargo ships as an obstruction to create NLoS maritime propagation. In addition, the stand-off distance has been introduced to analyze the NLoS propagation for surveillance applications. A ray tracing based simulator has been used to verify the measurement results and to identify and visualize the propagation paths. These studies classified the blockage ships into three types based on their structures, and then they have found the stand-off distance associated with each type. The results showed that when the blockage ship has complex periodic structures on top, the diffraction mechanism is more likely to take place. The multipaths from these structures causes the stand-off distance to get shorter. In the mentioned studies, the stand-off distance is defined as the shortest distance at which an Unmanned Surface Vehicle (USV) approaching a cargo ship, still can establish a trustworthy communication link with the control station on shore while the cargo ship is acting as an obstacle for the LoS path between transmitter and receiver.

Moreover, [21] and [23] used parabolic equations in the existence of evaporation duct to predict the propagation loss for frequencies above 2.5 GHz. However, the maximum

applied carrier frequency was 10 GHz. Since the complexity of parabolic equations is so high due to the final mathematical expressions include complicated exponential functions of Fast Fourier Transform (FFT) and Inverse Fast Fourier Transform (IFFT), this modeling approach could not draw the attentions. However, parabolic equations may follow the actual propagation loss pattern better than the other models.

The study done in [16] and [27] focus on time delay dispersion characteristics of mobile channels for the propagation over the sea at 5.8 GHz. They presented the measurement results for a series of instantaneous PDPs as well as analyzing the RMS delay spread as a small scale variations.

In [18], experiments at 5.8 GHz were carried out to investigate large scale and small scale variations over the sea. Based on their measurements, large scale fading can be modeled using classical log normal path loss models and small scale fading statistics fits the extreme value distribution (EVD) function when they are expressed in decibel units.

It should be noted that in [24], measured data have shown that large scale characterization of the marine channel depends highly on the antenna height.

In addition, among all studies done over the sea surface at the millimeter radiowaves, only a few of them have focused on small scale variations [11]-[13]. For instance, in [12] and [13], a series of measurement campaigns were initiated to accredit existing radar propagation models for different atmospheric conditions in the marine environment for millimeter radio waves. Although the path loss effect has been investigated very well in the mentioned studies, the small scale variations are left unexplained.

The studies [28]-[30] specifically focus on small scale variations of marine channel. Time dispersive parameters such as mean delay, RMS delay spread and coherence bandwidth have been extracted to decide whether the channel is frequency selective or not. Nevertheless the interested frequency of those studies is either 2 GHz or 5 GHz. Hereupon, there is the lack of a comprehensive study to address both small scale and large scale variations for millimeter radiowaves over the sea channel.

2.2 Existing Path Loss Models

One of the simple models that can be used for propagation loss prediction for maritime channels is the free space path loss (FSL) model which considers both antennas in the vacuum [18]. Based upon the FSL model, the propagation loss can be expressed as [19]

$$L_{FSL} = -27.56 + 20\log_{10}(f) + 20\log_{10}(d) \tag{2.1}$$

where f is the frequency in MHz, d is the separation between transmitter (TX) and receiver (RX) in meter, and L_{FSL} is the free space loss in dB. FSL model is valid only to prediction the exponentially increasing pattern of propagation loss without considering the effect of reflected ray from the see surface.

Another model often used as a reference is 2-ray model. This model takes into account two rays between a transmitter and a receiver including a direct ray and a reflected ray from the sea surface. For 2-ray model the path loss is given by [18], [31] as

$$L_{2-ray} = -20\log_{10}\left[\left(\frac{\lambda}{4\pi d}\right)\left|1 + a_v\exp(j\Delta\Phi)\right|\right] \tag{2.2}$$

where L_{2-ray} is the propagation loss in dB, λ is wavelength, d is the propagation distance, a_v is the reflection coefficient, and $\Delta\Phi$ is the phase difference between direct and reflected rays. In (2.2), if the angle of incidence with the sea considered to be close to grazing (i.e. the magnitude and the phase of the reflection coefficient are about one and 180°, respectively), 2-ray model can then be expressed as [19]

$$L_{2-ray} = -20\log_{10}\left\{\left(\frac{\lambda}{4\pi d}\right)\left[2\sin\left(\frac{2\pi h_t h_r}{\lambda d}\right)\right]\right\} \tag{2.3}$$

where h_t and h_r are transmitter and receiver heights in meter.

FSL and 2-ray analytical models will be used in Section 3.3 in order to predict the propagation loss for marine environment at 35 GHz and 94 GHz.

In the existence of evaporation duct, 3-ray path loss model is introduced including the effect of refracted ray due to the existence of duct height over the sea surface [19]. Then, it is concluded that for radio planning, near sea-surface LoS radiowave propagation loss,

L, in dB could be estimated generally as,

$$L_{3-ray} = \begin{cases} -20\log_{10}\left\{\left(\frac{\lambda}{4\pi d}\right)\left[2\sin\left(\frac{2\pi h_t h_r}{\lambda d}\right)\right]\right\}, d \leq d_{break} \\ \\ -20\log_{10}\left\{\left(\frac{\lambda}{4\pi d}\right)\left[2(1+\Delta)\right]\right\}, d \geq d_{break} \end{cases} \tag{2.4}$$

where $\Delta = 2\sin\left(\frac{2\pi h_t h_r}{\lambda d}\right)\sin\left(\frac{2\pi(h_e - h_t)(h_e - h_r}{\lambda d}\right)$, $d_{break} = \frac{4h_t h_r}{\lambda}$, and h_e is the effective ducting height. 3-ray model considers the refracted ray from the evaporation duct layer only after d_{break}. Hence, as it can be seen from (2.4), before d_{break}, 2-ray model is reliable even with the existence of evaporation duct.

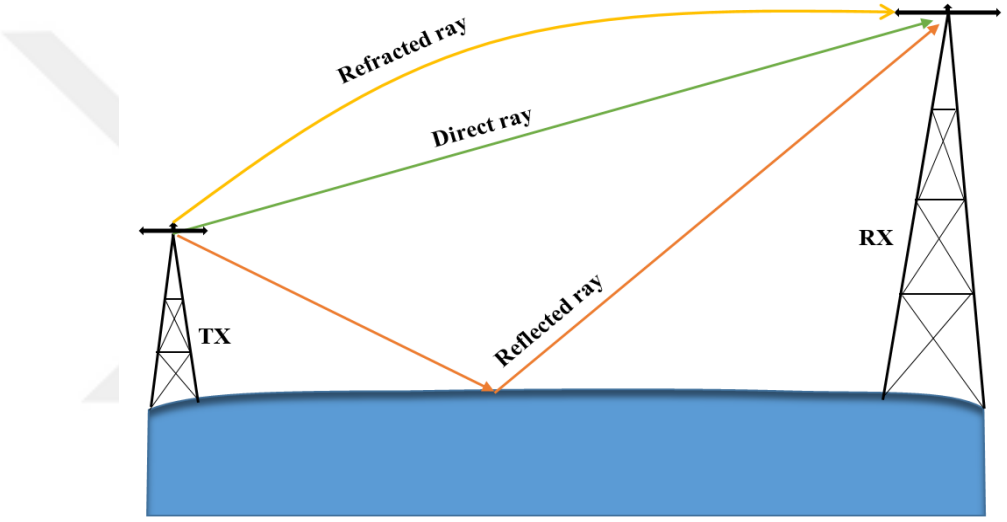

FIGURE 2.1: Maritime radiowave propagation with the existence of evaporation duct.

2.3 Chapter Conclusion

This chapter presented the survey performed by the authors for marine channel models at millimeter radiowaves. Different models for predicting the propagation loss over the sea surface have been investigated for different scenarios. The next chapter contains the discussion on the large scale variations for maritime environment at 35 GHz and 94 GHz. To the best of our knowledge, this is the first study that takes into consideration the effect of different parameters on large scale variation for ray tracing based channel modeling at the interested frequencies of 5G . Thereafter, small scale variations of channel will be discussed.

Chapter 3

Large Scale Variations

The previous chapter gave a quick overview on marine channel models as well as the path loss models that commonly used to predict the propagation loss over the sea channel. In this chapter, we will make a discussion on large scale variations and how different parameters can affect the channel over the sea surface. Then, a comparison between simulated and measured results will be performed to approve the accuracy of our channel modeling approach [1].

3.1 Methodolgy

In order to model the simulation environment, first we apply either "Full 3D Method" or "Vertical Plane" to create a 3-D environment as there are no objects except TX and RX over the terrain. In the second stage, we use Shooting and Bouncing Ray (SBR) method to trace the rays from the transmitters and propagating the rays through a desired environment unto the receivers. Those rays which hit building walls will be reflected specularly and keep moving to be traced up to the maximum number of interactions, or when the rays hit the terrain boundary. Interactions include reflections from the feature faces, diffraction around objects, and transmission through features. In the third stage, some parameters like path loss, ToA, and AoA are computed by simulator and then imported to Matlab® for more processes in order to obtain channel characteristics for

[1]The content of this chapter will be submitted for a potential IEEE journal

the environment under consideration. Figure 3.1 provides an overall summary of major steps followed in the channel modeling methodology.

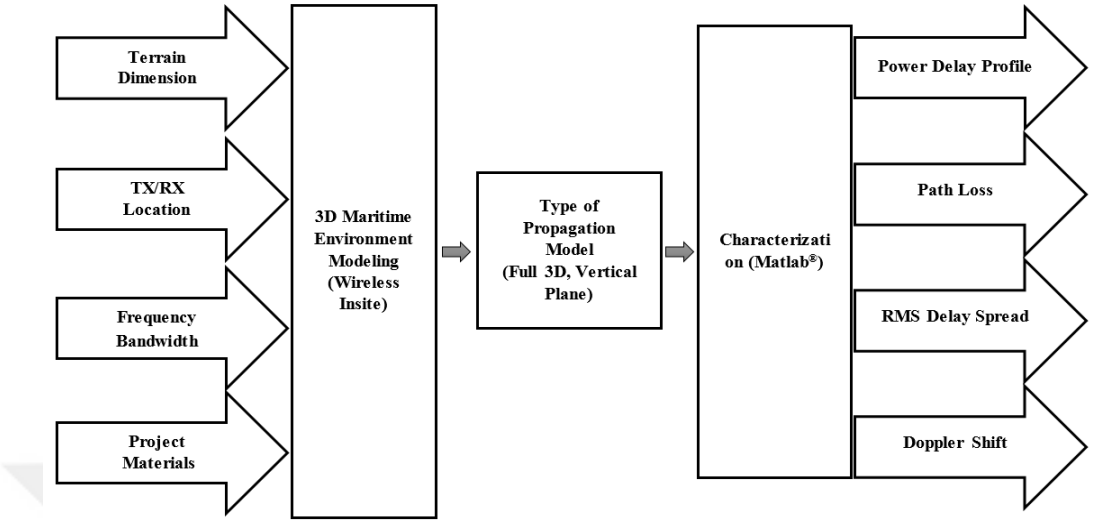

FIGURE 3.1: Steps in channel modeling and characterization.

3.1.1 Modeling of the Maritime Environment

In this section, we will review the main parameters which affect the channel model over the sea surface. These two parameters are evaporation duct height, which is dominant among the other ducts, and roughness of sea surface that strongly affects the signal strength specially at millimeter radiowave frequency band. Later, in section 3.2, we will consider them in our simulations and show how they mutate the maritime channel.

3.1.1.1 Duct Height

Maritime radiowaves propagation over is affected by different ducts such as elevated ducts, surface ducts, and evaporation ducts. Among the mentioned duct types, evaporation duct is dominant near the sea surface since there is a rapid decrease in vapor pressure from a saturation condition at the sea surface to an ambient vapor pressure at levels several tens of meters above the sea surface [19]. It has been demonstrated that the existence of evaporation duct height enhances the received signal strength significantly at frequencies greater than 3 GHz [32]. In addition, in [19] it has been shown that as the propagation distance increases beyond a certain point (i.e. d_{break}), evaporation duct causes an additional refracted ray to be received beside the direct and reflected rays from

the sea surface. Therefore, a multi-ray path loss model, which takes into consideration the signal trapped in the evaporation duct is introduced. Figure 3.2 illustrates the effect of distance between TX and RX on receiving the 3^{rd} ray. d_{break} can be approximately estimated as [19]

$$d_{break} = \frac{4h_t h_r}{\lambda} \tag{3.1}$$

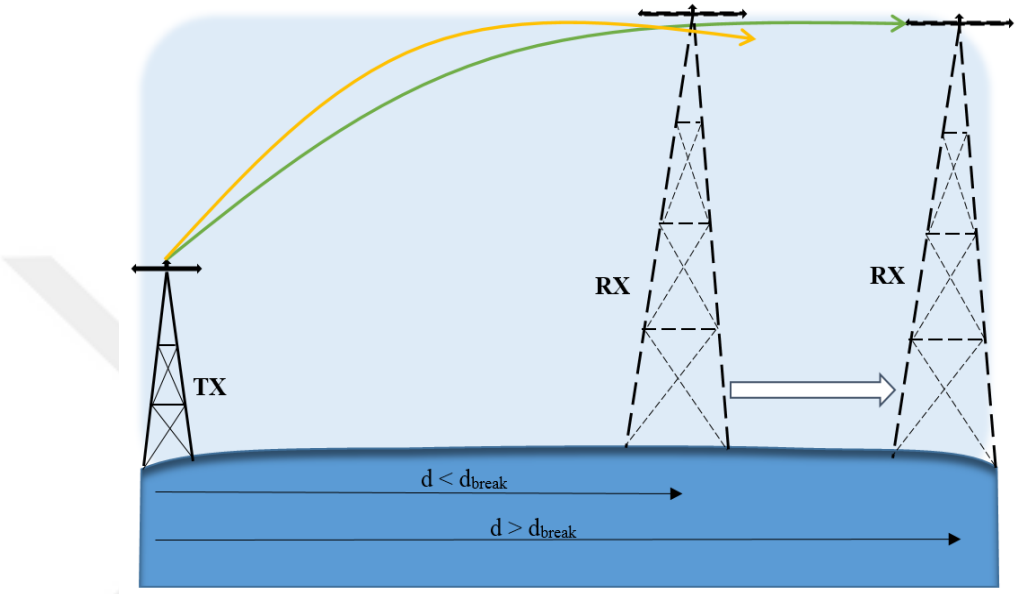

FIGURE 3.2: Effect of d_{break} on receiving the refracted ray due to the evaporation duct.

3.1.1.2 Roughness

In our simulations we assumed that over the sea, we are experiencing a calm situation and therefore, the wind speed is not high enough to change the sea surface roughness significantly [33]. Additionally, depends on location scenario that can be either onshore or offshore, the related roughness will be different. In onshore scenarios [33], since we have too many vehicles (e.g., vessels, boats, etc), in such a small region, the vehicle's movement causes billows and results in a higher value of roughness, which which cannot be zero anymore. In [32] sea states have been divided into 9 different categories based on the roughness diversity. In each state, a boundary of roughness is introduced to mention the minimum and maximum height of waves. Since we assumed a calm situation is being experienced, sea state number zero should be considered in our simulations which has maximum 1 ft wave height. However, in Section 3.2, we will take into account different roughness values to observe the effect of roughness on the maritime channel. Figure 3.3

shows the effect of sea surface roughness on the angle of reflection, and consequently, the reflection coefficient.

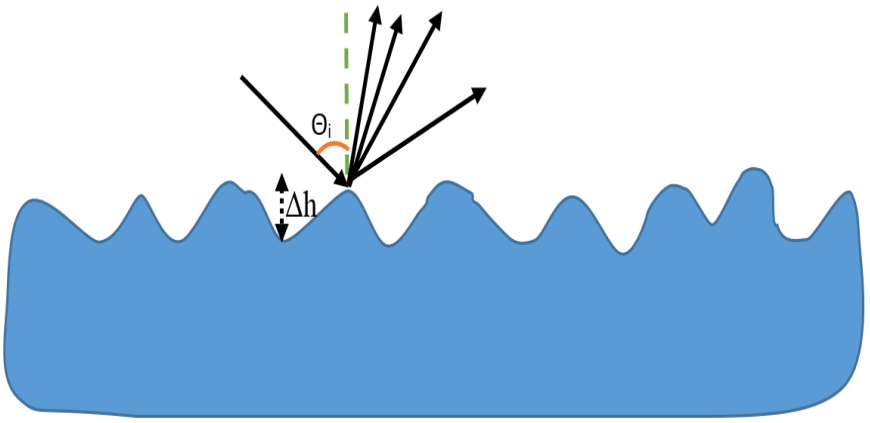

FIGURE 3.3: Effect of roughness on the reflection coefficient.

3.1.2 Type of Propagation Model

Wireless InSite provides several ray-based propagation models such as Full 3D, Urban Canyon, and Vertical Plane. These models all combine ray tracing algorithms with UTD. The ray tracing approach is applied to find the propagation paths moving toward each receiver while UTD is used to evaluate the complex electric field associated with each ray path. In this study, both Full 3D and Vertical Plane methods are used for different purposes. The Full 3D method in the software also allows propagating the rays across the simulated terrain considering the effects of transmission, reflection, and diffraction on the electric field. However, in order to consider the curvature of Earth, we use Vertical Plane method which includes the effects of Earth's curvature in its calculations by employing a 4/3 Earth radius correction. This is the default Earth's curvature setting, and may be deactivated. It should be noted that this method is very helpful to save the run time whenever we are going to account the Earth's curvature. Otherwise, the simulation will take long time to run.

In this study, there are only two dominant rays including direct ray from the transmitter to the receiver and reflected ray from the sea surface. The effect of 3^{rd} ray, corresponding to the refracted ray from the evaporation duct height, is negligible since the separation of TX and RX does not exceed d_{break} in our framework setup. Figure 3.4 illustrates the LoS and sea surface reflected rays within the terrain.

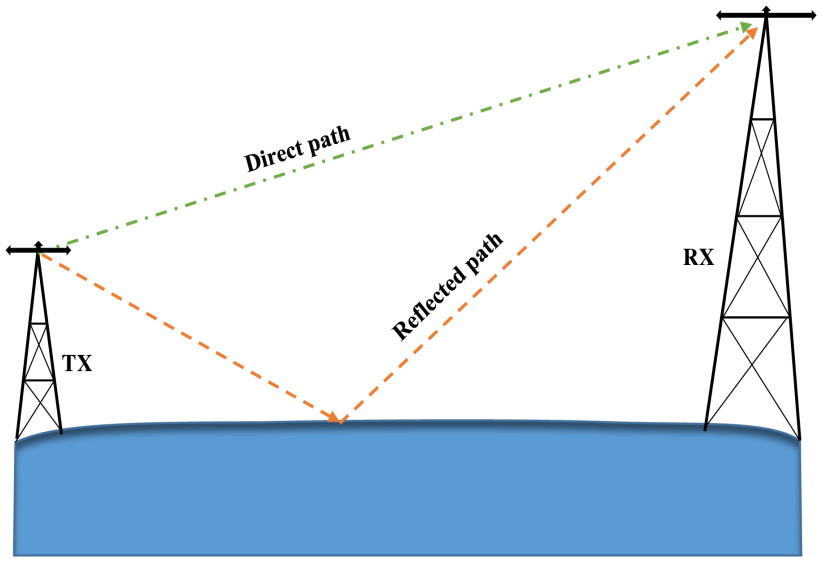

FIGURE 3.4: Near sea surface radiowave propagation.

3.2 Effect of Different Parameters on Maritime Channel Models

In this section, based on our methodology, we present channel characteristics for two different frequencies. We also investigate the effect of ray spacing, Earth's curvature and sea surface roughness on maritime channel models. Since we consider 35 GHz and 94 GHz frequency bands, d_{break} would be around 23 km and 61 km, respectively. Hence, if we assume that the longitude of terrain is 20 km, which is even less than the break distance of 35 GHz, evaporation duct does not have a significant effect and hence we still might use Full 3D or Vertical Plane propagation models. We consider a transmitter height of 5.63 m while its power is chosen to be 23 dBm. The receiver is assumed to have a height of 20 m at different distances from the transmitter. It should be noted that LoS was maintained throughout the simulations. The main parameters of the scenario under the consideration are summarized in Table 3.1 [11]-[12].

3.2.1 Effect of Ray Spacing

After creating a scenario by including the terrain material, transmitter-receiver locations and heights, etc., the secondary parameter to be considered is the ray spacing relative to the geometry. The spacing should be small enough that at least two rays intersect

TABLE 3.1: Simulation parameters of scenario under consideration

Parameter	**Value**
Carrier Frequency	35 GHz - 94 GHz
Bandwidth	200 MHz
Transmitted Power	23 dBm
Transmitter Height	5.63 m
Receiver Height	20 m
Terrain Dimension	20 km × 1 km
Sea Permittivity	20 Farads/m
Sea Conductivity	81 Siemens/m
Transmitter Antenna	Directional
Receiver Antenna	Omnidirectional
Polarization	Vertical

the majority of facets in line of sight of the receiver. The condition is commonly satisfied when considering the ray spacing relative to the collection surface, but in some instances, this condition, i.e. receiving at least two rays at all receiver locations, can be the determining factor in choosing ray spacing. The "ray spacing" entry is a value in degree and it is defined as the space between adjacent ray paths during the ray tracing. The proper setting for this parameter depends on several factors including the size of the project, the size of the facets in the project, and the distance of the facets from the transmitter. The default value of ray spacing in Wireless InSite simulator is 0.25°. However, by increasing the simulated area, ray spacing should be decreased to have more realistic channel model and prepare the "minimum conditions" in which, the receiving of the second ray is feasible. In our study presented in [34], we have considered 0.2° ray spacing and based on that, we introduce a proposed model which is a modified version of 2-ray path loss model[2]. This particular study, tried to propose a new model that cancels the extra peaks introduced by 2-ray analytical model due to the power of exponential function. Also in our model, we do not consider simplifications such as incidence angle being too small. Our proposed model for prediction of propagation loss is as follows:

$$L_{m2-ray} = -20\log_{10}\left\{(\frac{\lambda}{4\pi d})\left|1 + R\exp(j\frac{\alpha 2\pi\Delta d}{\lambda})\right|\right\} \tag{3.2}$$

[2]This channel model has been accepted by The 24th International Conference on Software, Telecommunications and Computer Networks (IEEE SoftCOM2016) with the name "Novel Maritime Channel Models for Millimeter Radiowaves"

where λ, d, and Δd are wavelength, distance between TX and RX, and the difference between the two ray paths, respectively. The expression Δd can be obtained in a straightforward manner as

$$\Delta d = \sqrt{(h_t + h_r)^2 + d^2} - \sqrt{(h_t - h_r)^2 + d^2} \tag{3.3}$$

Also, because the roughness assumed to be zero, R, reflection coefficient, is equivalent to "-1". Although, there exists an exact relationship between roughness and reflection coefficient for the low frequencies such as underwater acoustic [35], to the best of our knowledge, for the high frequencies no exact relation has been expressed. In (3.2), α is a unit-less coefficient that is obtained by minimizing the least square error of simulation results and the results predicted by the proposed model. α is around 0.17 and 0.06 for 35 GHz and 94 GHz, respectively.

To observe whether the proposed model is reliable even for the low frequencies, we used our model for 5.15 GHz and found α as 0.98, a very close number to 1. Therefore, our model reduces to 2-ray analytical model when the frequency is low. Since α is dependent on the frequency, it can be seen that by increasing the frequency (e.g., frequencies greater than 1 GHz), α decreases exponentially. Through least-square error minimization, α can be expressed as

$$\alpha = 1.091 \exp\big(-0.06256 f\big) + 0.06982 \tag{3.4}$$

where f is the frequency in GHz. The root mean square error (RMSE) between the actual and estimated alpha value is 0.0434. It should be noted that for the low frequencies less than 1 GHz, α can be set to unity.

Towards better understanding of the proposed model, we make a comparison with the existing analytical models . In Figure 3.5, we present the path loss versus distance for 35 GHz, 94 GHz, and 5.15 GHz. We have also demonstrated the path loss for 5.15 GHz, since it is a popular band for WiMAX applications for marine channels. It is observed that although there is a good agreement between 2-ray path loss model and simulated results for lower frequencies (Figure3.5c), for high frequencies such as 35 GHz and 94 GHz, both models are unable to model the maritime channel even for transmitter/receiver separations less than d_{break}. However, for short ranges (almost less than 2 km), still 2-ray model is applicable [18].

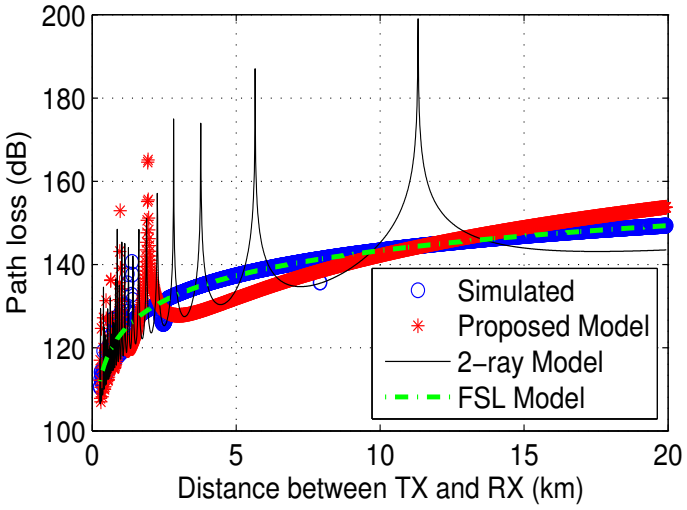

(a)

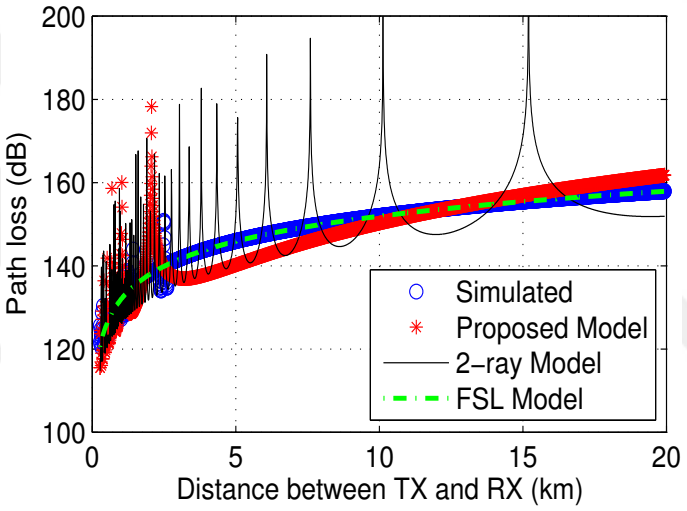

(b)

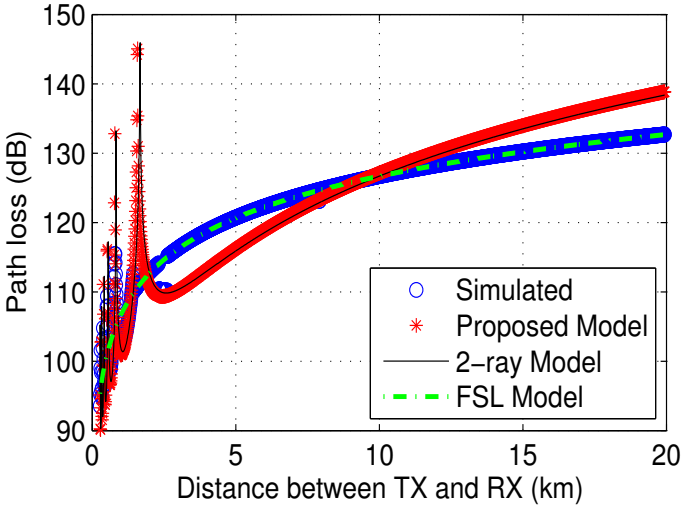

(c)

FIGURE 3.5: Path loss versus distance at different frequencies; (a) at 35 GHz (b) at 94 GHz (c) at 5.15 GHz.

It should be noticed that the FSL model can only predict the exponentially increasing trend of propagation loss. In the other word, FSL model is appropriate only to predict the local mean of propagation losses [19]. Our results demonstrates that the proposed model can predict the last peak of path loss very well without introducing some other extra peaks considered through 2-ray path loss analytical model. It is also observed that the propagation loss model for high frequencies can be better predicted with the proposed model.

As a rule of thumb, for a 500 m $\times$ 500 m area, we should use at most 0.2° of space between the rays [31]. Since in our configurations, terrain area is chosen to be 20 km $\times$ 1 km, the ray spacing has to be at most 0.0025°. In Figure 3.6, the separation of transmitter and receiver (d) can be expressed as

$$d = d_1 + d_2 = (h_t + h_r)\tan(\alpha) \tag{3.5}$$

By considering 0.25° as the ray space, the maximum possible value that can be assigned to α in such a way that the transmitted ray hit to the sea surface and reflect from is 89.75°. Hence, the maximum distance between the transmitter-receiver pair that the reflected ray can be received is

$$d_{max} = (5.63 + 20)\tan(89.75) \tag{3.6}$$

that is roughly about 5.874 km. In fact, by choosing the default ray spacing of the simulator, which is 0.25°, we are blocking the reflected ray to be received after d_{max}. While by choosing a small ray spacing value (i.e. 0.001°), d_{max} will be increased to about 842 km and hence, our terrain dimension will be covered completely. In order to show how this parameter significantly affects the channel model, path loss curves for two different ray spacing values (i.e. 0.25° and 0.001°) at both 35 GHz and 94 GHz frequencies have been illustrated in Figure 3.7.

Figure 3.7 represents that by decreasing the ray spacing we observe more fluctuations due to the reflected ray from the sea surface. In the other words, whenever the ray spacing is small enough to make d_{max} larger than the terrain longitude, even at large distances, the second ray (i.e. reflected ray from the sea surface) can be received at the receiver side.

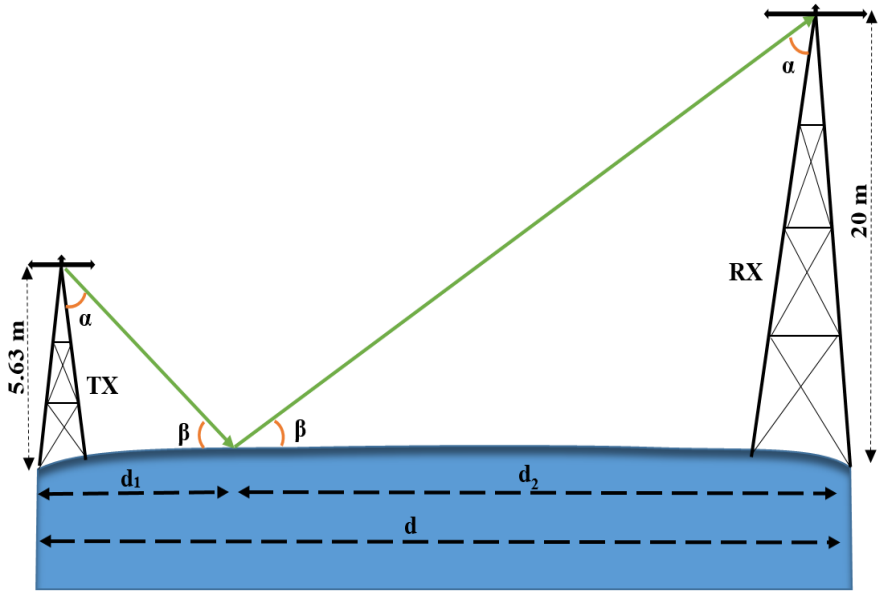

FIGURE 3.6: Scenario under the consideration for large scale variations.

Figure 3.8 shows that by decreasing the ray spacing, in some large distances, RMS delay spread increases. This observation is due to the fact that when the ray spacing is decreased, receiver catches the reflected ray from the sea surface at some longer distances. The delay associated with this reflected ray is added to the direct ray's delay and makes the delay spread greater by around 5 nsec. Therefore, by increasing the distance, RMS delay spread of 0.001° ray spacing becomes more than that of for 0.25° ray spacing. However, in the short distances, RMS delay spreads of both ray spaces are almost the same. Thus, to have more reliable channel models, we need to decrease the ray spacing at a cost of increasing the simulation run time. In Sections 3.2.2 and 3.2.3, we investigate the effect of other parameters such as Earth's curvature and sea surface roughness on the channel model over the sea surface.

3.2.2 Effect of Earth's Curvature

In this section, we investigate the effect of Earth's curvature to see how this parameter affects the channel parameters. As it is mentioned in Section 3.2.1, in order to have more realistic channel models, ray spacing should be chosen as 0.001° in our simulation setup. However, decreasing the ray spacing, increases the accuracy at the cost of longer run time. Therefore, using another propagation model, named as "Vertical Plane", is suggested to decrease the run time as well as including the Earth's curvature effect [14].

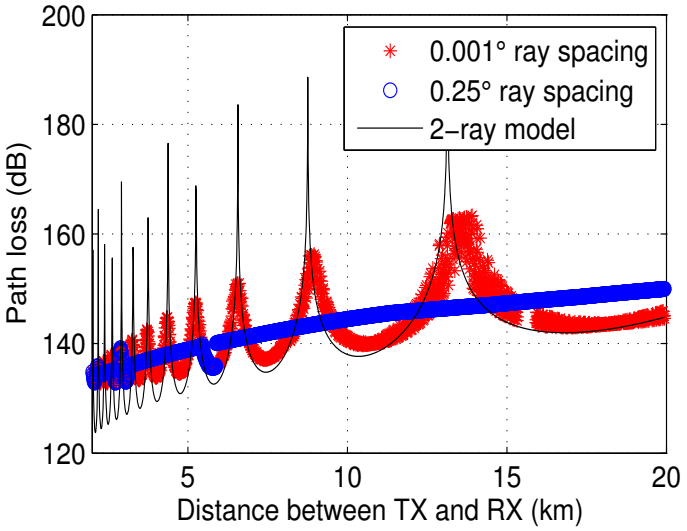

(a)

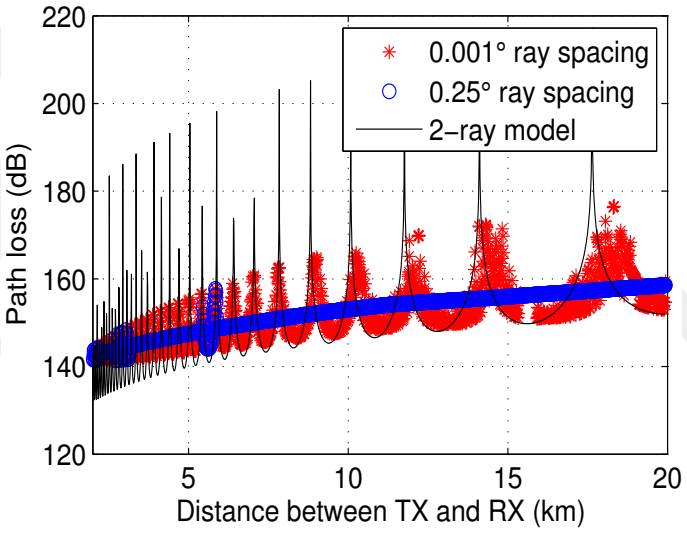

(b)

FIGURE 3.7: Effect of ray spacing on the path loss; (a) at 35 GHz and (b) at 94 GHz.

The Vertical Plane model is a ray-based propagation model that traces all paths from the transmitter within a two-dimensional vertical plane. It is primarily intended for predicting propagation over irregular terrain at the interested frequencies of very high frequency (VHF) and ultra high frequency (UHF). Vertical Plane keeps information about all propagation paths including the time and direction of arrival for various contributions. For the free space cases, the Vertical Plane model results are ideal, with only the antenna radiation pattern and distance impacting the channel parameters. For the environment with ground or water, Vertical Plane applies material properties through the reflection

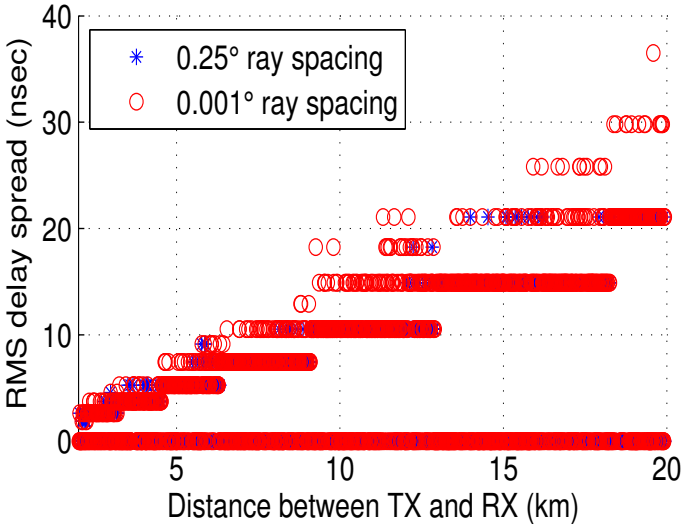

(a)

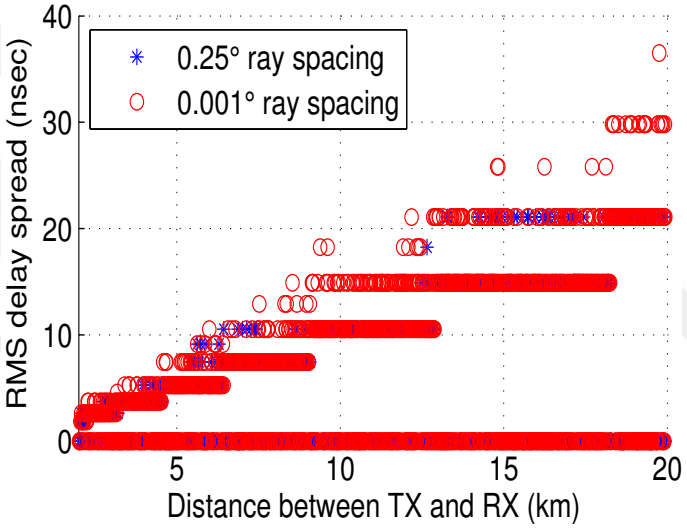

(b)

FIGURE 3.8: Effect of ray spacing on RMS delay spread; (a) at 35 GHz and (b) at 94 GHz.

coefficients when the ray paths intersect and interact with a surface. It handles reflections and multiple diffraction through the application of Geometric Optics (GO) and UTD.

We have already mentioned in Section 3.1.2 that Vertical Plane propagation model includes the effect of Earth's curvature by applying 4/3 Earth radius correction. Based on the results obtained from the simulator, when we are considering the Earth's curvature, in some large distances, more than two rays can be received due to the diffraction around the Earth.

Based on the observations, the first diffracted ray was received beside the direct and reflected rays at about 4.8 km, and up to 6 rays have been received after about 16 km away from the transmitter. Most of these received rays had experienced minimum 0 and maximum 2 times diffraction. The first received ray was LoS ray, second one was reflected ray from the sea surface, after that one or two rays, which had first order diffraction and finally ray or rays with second order diffraction have been received at the receiver side. Hence, by increasing the separation of transmitter and receiver, we are actually increasing the number of received rays (beside LoS and reflected ray) that experienced either first or second order diffraction.

Another important issue to be mentioned is that by choosing the 0.25° ray spacing in the simulations, we may not see the Earth's curvature effect since any other ray except LoS is blocked after about 6 km for this amount of ray spacing. This observation proves that applying the 2-ray analytical path loss model would not be sufficient for predicting the propagation loss at the large distances over the sea surface because of the existence of other diffracted rays due to the Earth's curvature.

Figure 3.9 illustrates the propagation loss with and without considering the Earth's curvature effect. It can be seen that after about 12 km more diffracted rays are received and path loss value decreases. Also, analytical 2-ray model has been shown on the figure to be compared with the simulated path losses. As it can be seen in Figure 3.9, by increasing the distance, 2-ray analytical model is losing its ability to predict the simulated path loss values.

From Figure 3.10, it is observed that although at short ranges RMS delay spread is the same for flat and curved terrain, by increasing the distance, RMS delay values would be greater by considering the Earth's curvature. This difference, which is around 10 nsec, is due to receiving more rays beside the direct and reflected rays at some larger distances. It should be noticed that at some distances, RMS delay is the same for both terrains (i.e. flat and curved terrains), since at some distances, even larger than 4.8, it is possible not to receive the diffracted ray. In the other words, under the consideration of Earth's curvature, if more than two rays (i.e., direct and reflected rays) been received at the receiver side, we expect the RMS delay spread to be different than the value obtained for flat terrain; Otherwise, the RMS delay spread values would be the same. In the next section, we will consider the effect of surface roughness on the sea channel.

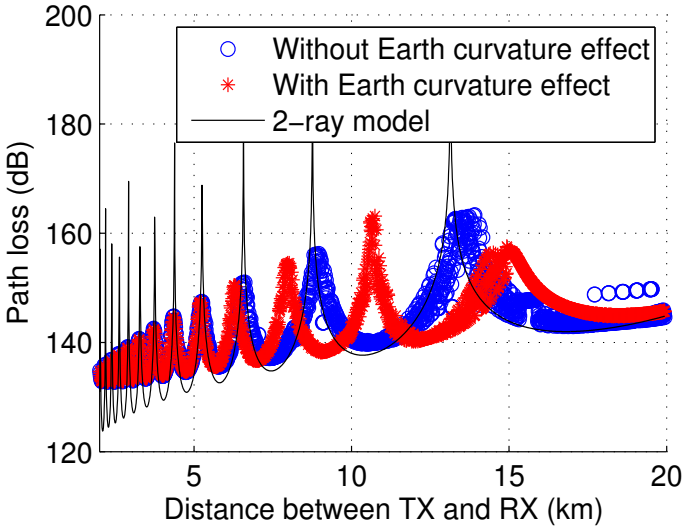

(a)

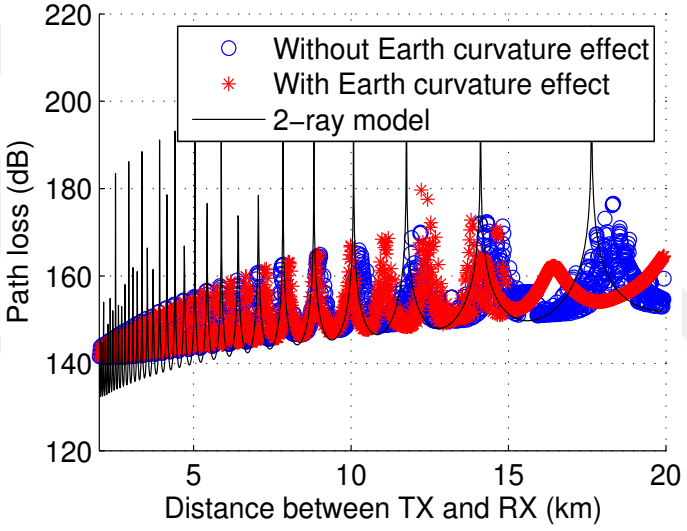

(b)

FIGURE 3.9: Effect of Earth's curvature on the path loss; (a) at 35 GHz and (b) at 94 GHz.

3.2.3 Effect of Sea Surface Roughness

As it has been discussed in the previous sections, the ray space should be about 0.001° in our simulation. In addition, Earth's curvature has significant influence on the propagation model and therefore the inclusion of this effect is necessary in order to have more realistic channel model.

In this section, we will discus the effect of sea surface roughness, which is another important factor beside the ray spacing and Earth's curvature in the maritime environment

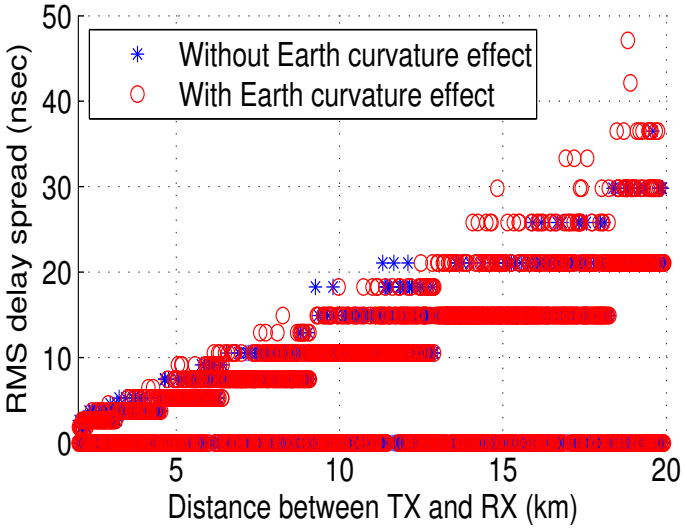

(a)

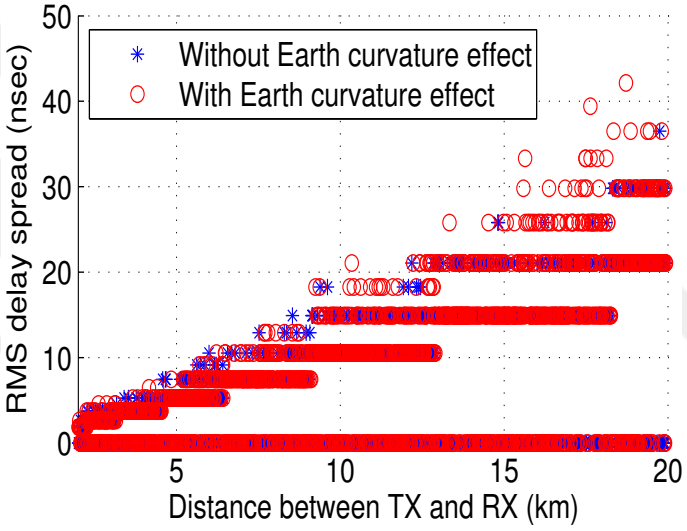

(b)

FIGURE 3.10: Effect of Earth's curvature on the RMS delay spread; (a) at 35 GHz and (b) at 94 GHz.

simulations. Roughness can be defined as the standard deviation of the surface height relative to the mean height, in meters [14]. To account for the decrease in the reflected energy in the specular direction, the reflection coefficient for a rough surface is determined by using:

$$R = R_0 \exp\left[-8\left(\frac{\pi(\Delta h)cos(\theta_i)}{\lambda_0}\right)^2\right] \tag{3.7}$$

where R_0 is the smooth surface coefficient, θ_i is the angle of incidence, Δh is the standard deviation in the surface height around the mean height, and λ_0 is the wavelength [14]. In 2-ray analytical path loss model, the reflection coefficient, R, is assumed to be -1 for all

surfaces regardless the surface material or applied frequency, and this is another weakness of 2-ray model application over the sea surface. It was mentioned in Section 3.1.1.2 that we assumed a calm situation with sea state number zero case. Under these assumptions, sea surface has maximum 1 ft wave height. To see the effect of roughness, first we assume that there is no roughness over the sea surface, and then we increase this amount to 1 ft (or 0.3048 m).

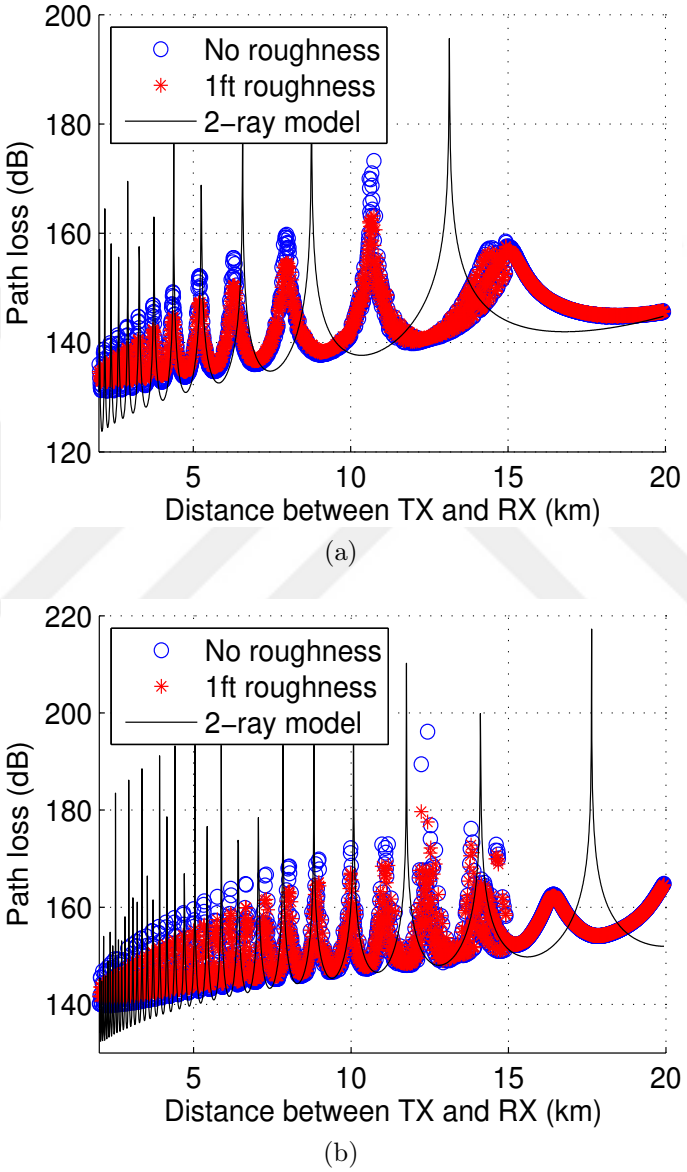

FIGURE 3.11: Effect of sea surface roughness on the path loss; (a) at 35 GHz and (b) at 94 GHz.

Figure 3.11 demonstrates the simulation results for the sea channel without surface roughness and with 1 ft roughness at 35 GHz and 94 GHz. It can be observed from Figure 3.11 that for the sea without surface roughness, the fluctuations are sharper than that of for

1 ft roughness since the roughness is changing the reflection coefficient from the sea surface. However, the roughness does not change the location of peaks in the path loss pattern; it just makes the fluctuations smoother. In another words, by considering the sea surface roughness, the overall pattern of path loss does not change, and only the power loss will be changed especially at short distances between the transmitter and the receiver. In order to show how this property (i.e. roughness) affects the RMS delay spread, Figure 3.12 has been generated.

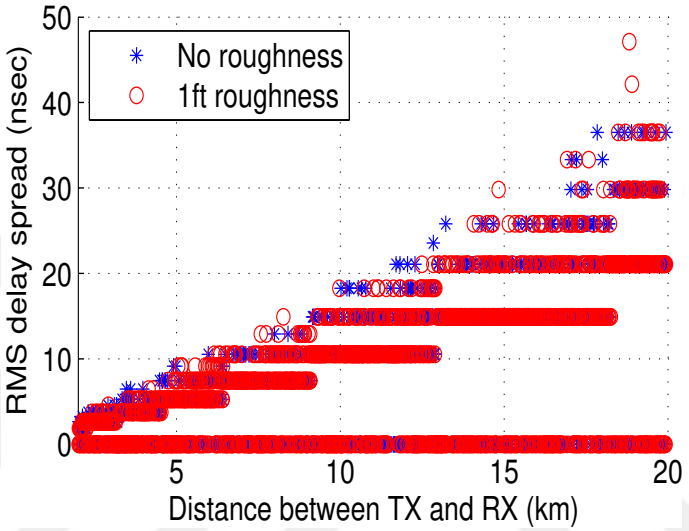

(a)

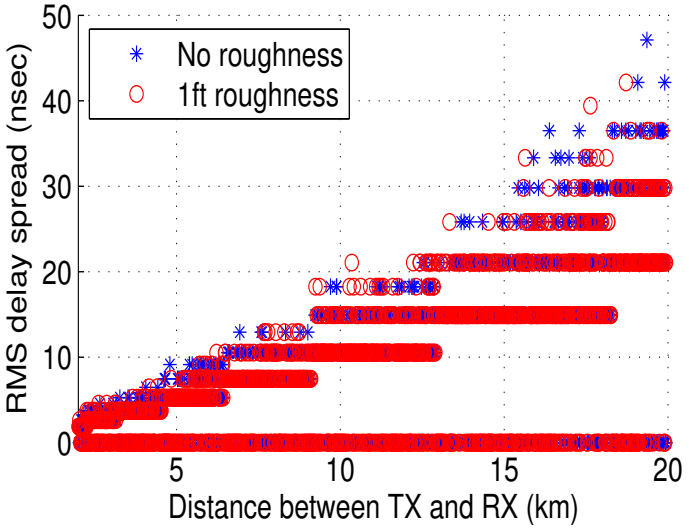

(b)

FIGURE 3.12: Effect of sea surface roughness on the RMS delay spread; (a) at 35 GHz and (b) at 94 GHz.

From Figure 3.12, it is deduced that inclusion of the roughness into the channel model does not change the RMS delay spread significantly. Though, at 94 GHz, more differences

can be observed between the RMS delay spread pattern with and without the roughness. This notable difference is due to the very short wavelength at 94 GHz, which is performing an effective rule in (3.7), reflection coefficient equation.

3.3 Comparison with the Measurement Results

As it is already discussed, there have been only some sporadic efforts to address maritime channel modeling at millimeter radiowaves [12]-[13]. In this section, we will perform a comparison between our simulated results and the measured study presented in [13].

To make a one-to-one comparison, we consider the same environment and parameters of [13]. For the sake of simplicity but without loss of generality, in our simulations, the terrain longitude is 20 km to make sure the evaporation duct has no effect on the channel and the duct height is negligible. The applied frequencies are 35 GHz and 94 GHz with 200 MHz bandwidth. The transmitter and receiver antennas are directional and omnidirectional, respectively. It should be noted that at 35 GHz the beam width of transmitter is 1.1°, while at 94 GHz the beam width is 0.8°.

It can be seen from Figure 3.13 that the simulated results follow the measured data at both frequencies almost everywhere. However, in the study done by [13], due to a lack in accurate definition of the sea surface roughness, some mismatches observed especially at 94 GHz. In the next section, we will show how the roughness affects the channel model in ray tracing based simulations.

3.4 Chapter Conclusions

In this chapter, an investigation of over the sea surface LoS millimeter radiowave propagation at two different frequencies (i.e., 35 GHz and 94 GHz) is discussed. We investigated the effect of varying distance between the transmitter and receiver on path loss, received power, and RMS delay spread. Our results demonstrated that for high frequencies such as 35 GHz and 94 GHz, both analytical models (i.e., 2-ray and FSL) are unable to model the channel over the sea surface. It is observed that for short ranges, prediction of 2-ray model is still reliable, however. Besides, FSL model can only predict the exponentially increasing of propagation loss at both applied frequencies. Our results additionally showed

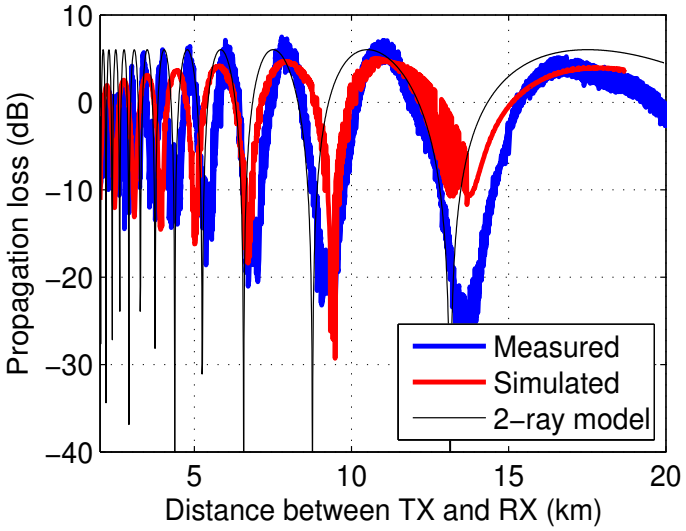

(a)

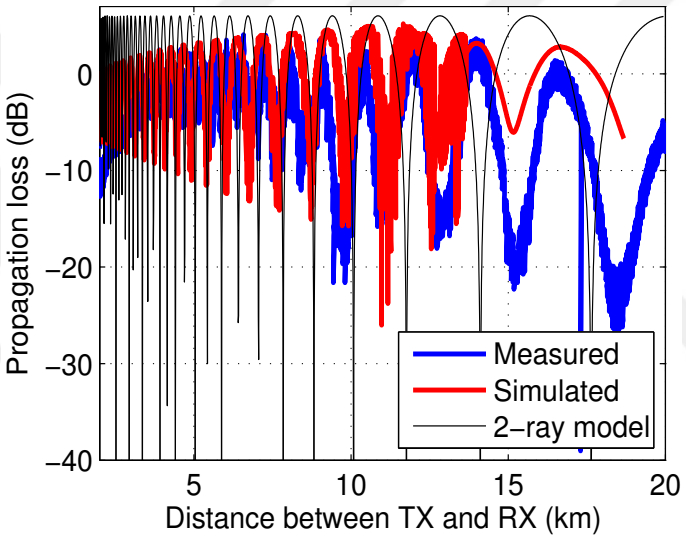

(b)

FIGURE 3.13: Comparison of measured data with simulated results; (a) at 35 GHz and (b) at 94 GHz.

that 2-ray analytical propagation loss model should only be used for short ranges over the sea surface at typical frequencies considered by 5G, and FSL model cannot predict the behavior of channel over the sea surface in high frequencies even for short ranges.

Based on our proposed modelling approach, ray spacing is a very important factor to have more realistic channel models in ray tracing based channel simulators. This parameter should be specified small enough to at least two rays been received at the receiver in almost all RX locations.

In addition, the terrain shape is another factor which highly affects the simulated results. By considering the Earth's curvature, propagation loss will be decreased as more paths are received at larger distances due to the diffraction around the Earth. However, because of receiving more paths (i.e. diffracted paths) associated with more delays, RMS delay spread values would be greater at some distances in which diffracted rays were received beside LoS and reflected rays at the receiver. Although, ray spacing and Earth's curvature both highly affect the channel parameters, sea surface roughness does not change the propagation loss pattern significantly. Roughness affects how sharply the fluctuations occur in path loss model. However, the earlier property, causes a little differences in RMS delay spread pattern.

Chapter 4

Small Scale Variations

After that the previous chapter has explained the large scale variations of channel by considering the effect of different parameters, this chapter will illustrate the small scale variations such as RMS delay spread and Doppler frequency[1].

4.1 Methodology

In order to determine the small scale variations of maritime channel model, we use the methodology introduced in the previous chapter. First of all, we need to create a 3D environment with the specific properties of marine scenario such as conductivity, permittivity, and roughness. In the next step, we choose SBR method which traces the rays from a transmitter and then propagates the rays through a defined environment until they reach a receiver. The rays, which are specularly reflected, have at most 30 interactions. These interactions include transmission, reflection, and diffraction around the objects. In the final step, the raw data obtained by the simulator will be imported to Matlab® for more analysis to compute the channel properties such as Doppler and RMS delay spreads. A 4/3 Earth radius correction has been employed in the simulation tool to account for the effect of Earth's curvature. In addition, although the evaporation duct height is dominant among the other duct heights over the sea environment, since

[1]This study has been accepted by International Black Sea Conference on Communications and Networking (IEEE BlackSeaCom2017) with the name "Multipath Delay Profile and Doppler Spread of Millimeter Radiowaves over the Sea Channel"

the maximum separation of TX and RX sides is not large enough in our scenario, the effect of duct height is negligible [19], [34].

Figure 4.1 illustrates the scenario under consideration over the sea surface. In our scenario, the transmitter is fixed at the left-top of the environment plan while the receiver is moving from the middle left point to the middle right point of terrain. In our simulations we assumed over the sea channel to experience a calm situation or zero state sea condition [33]. Since the maximum roughness that can occur for zero state is 1 ft, we have specified 0.3048 m roughness in our simulations, which is equivalent to 1 ft roughness. To consider the decrease in the reflected energy in the specular direction, the reflection coefficient for a rough surface is determined by 3.7.

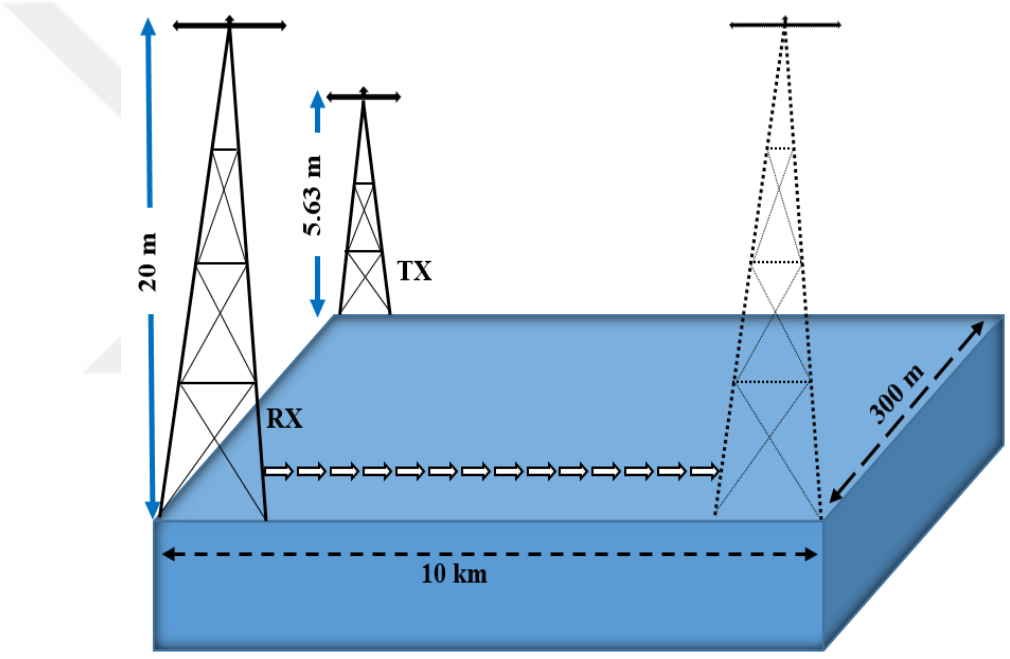

FIGURE 4.1: Over the sea scenario under the consideration for small scale variations.

4.2 Channel Characteristics

Based on our methodology, in this section we present the time delay domain parameters as well as the Doppler spread for the maritime scenario for two different frequency bands, *i.e.*, 35 GHz and 94 GHz. Based on the measurement campaigns reported, which used the mentioned frequencies for marine environments [12], [13], the bandwidth in our study is chosen to be 200 MHz.

The transmitter and receiver heights are 5.63 m and 20 m, respectively. The transmitted power is 23 dBm and both transmitter and receiver antennas are omnidirectional. Since the average speed of a typical ship is between 12 knot and 28 knot [36]-[37], in our study, we take 28 knot as the maximum average receiver speed to see how this speed affects the channel. Notice that the distance between each consecutive receiver locations is 10 m, and maximum separation of transmitter and receiver is going to be 10 km.

4.2.1 Mean Delay and RMS Delay Spread

Based on our simulated results, about 4 to 7 paths with different delays arrive at each receiver location. As an example, PDPs of the start point and the middle point (corresponding to 1 sec and 682 sec after the receiver ship begins to move) have been shown in Figure 4.2 for 35 GHz and 94 GHz. Figure 4.2 shows that at the start point which receiver is exactly in front of the transmitter. The dominant path is the direct path and the other received rays have almost 30 dBm less power than the direct path's power.

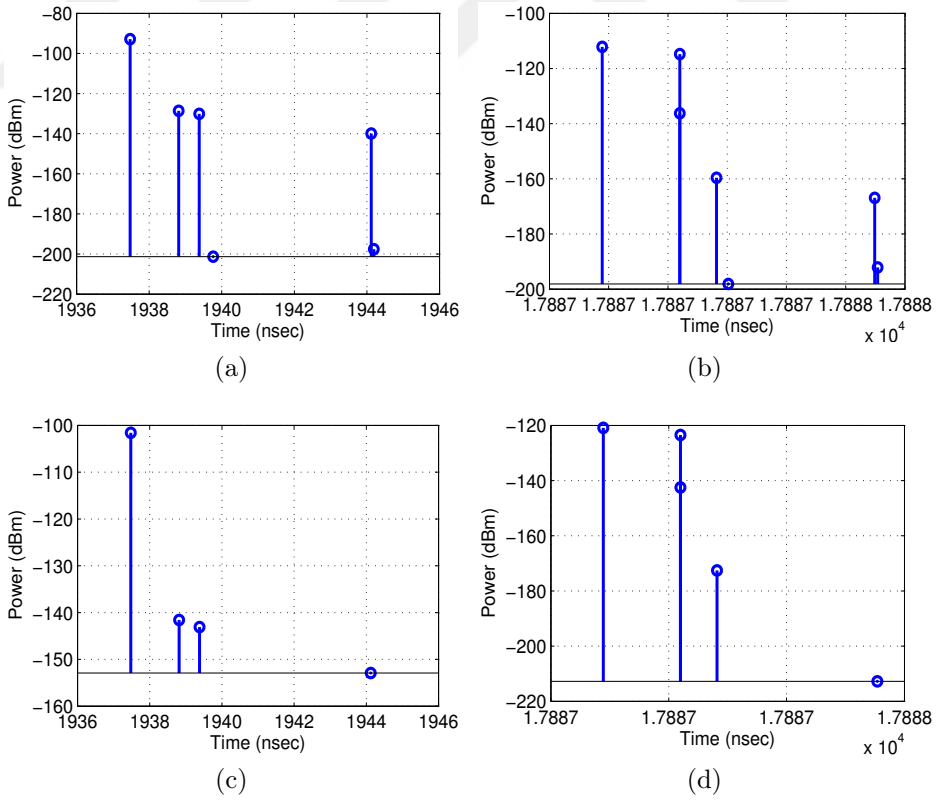

FIGURE 4.2: Power delay profiles at different times/locations and various frequencies; (a) at 35 GHz after 1 sec, (b) at 35 GHz after 682 sec, (c) at 94 GHz after 1 sec, and (d) at 94 GHz after 682 sec.

However, the PDP at the middle way indicates that the power of reflected and first diffracted rays are close to the direct ray's power. Nonetheless, in the earlier position, direct path has more power compared to other paths. Further, Figure 4.2 illustrates that the overall PDP shape at each time/location is the same for 35 GHz and 94 GHz; except that the received power at 35 GHz is about 10 dBm less [34]. It should be noted that the PDPs have the spiky shape which is expected due to the character of maritime environment [30]. This result is remarkably different than those results expected from indoor and urban areas.

From the average PDPs obtained at each receiver location, statistical properties of the mean excess delay (T_m) and RMS delay spread (σ) can be estimated from [29] as

$$T_m = \frac{\sum_{i=1}^{N} p_i t_i}{\sum_{i=1}^{N} p_i} \tag{4.1}$$

$$\sigma = \sqrt{\frac{\sum_{i=1}^{N} p_i {t_i}^2}{\sum_{i=1}^{N} p_i} - {T_m}^2} \tag{4.2}$$

where p_i denotes the power amplitude value at the discrete time instances t_i in multipath structure of PDP. Since the bandwidth at 35 GHz and 94 GHz assumed to be same (200 MHz), T_m and σ are almost the same at these two frequencies. As an example, the main parameters of time delay domain for the configurations shown in Figure 4.2 have been summarized in Table 4.1.

TABLE 4.1: Summary of time delay parameters for Figure 4.2 configurations

Configuration	T_m **(μsec)**	σ **(nsec)**
(a) and (c)	1.9621	0.0339
(b) and (d)	17.8871	0.0627

All simulated results presented above are related to a single receiver position and we have not discussed about the overall survey including the key channel parameters of probabilistic distributions.

Figure 4.3 shows the cumulative distribution functions (CDFs) for the mean excess delay, RMS delay spread, and 90% coherence bandwidth for both frequencies of interest. Based on the Figure 4.3, the RMS delay spread values are in nsec order, which means the reflections from the environment are similar to LoS in the delay domain. In addition, the RMS delay spread values are low enough not to have frequency selective channels. Also

in the frequency domain, we can observe that the 90% coherence bandwidths at 35 GHz and 94 GHz are 744 MHz and 1.53 GHz, respectively. These results may confirm the conclusion stated above about low RMS delay spread values of these two frequencies for marine environment. In other words, the results of 90% coherence bandwidths are further evidence for experiencing frequency non-selective maritime channel for this scenario. Although the 90% values of mean excess delay and RMS delay spread are exactly the same for both frequencies, 90% value of coherence bandwidth is not the same for 35 GHz and 94 GHz. The reason can be explained based on the RMS delay spread results shown in Figure 4.3b. For the small RMS delay spread values, the CDF of 35 GHz is not exactly the same as that of 94 GHz. These small values will be large when they get reversed to compute the corresponding coherence bandwidth. Therefore, the CDF would be different at wide coherence bandwidths and it affect 90% value of B_c. Table 4.2 summarizes the key results of channel parameters. Based on the results shown in Table. 4.2, it is possible

TABLE 4.2: Key maritime channel parameters

Parameter	50% value	90% value
T_m (μsec)	17.89	31.01
σ (nsec)	0.05067	0.09917
B_c (GHz) at 35 GHz	0.3946	0.7448
B_c (GHz) at 94 GHz	0.3946	1.53

to have high data rate transmissions without using a complex communication system over the sea channel under consideration [30].

4.2.2 Doppler Spread

Next we will show the effect of receiver speed over the sea surface, which causes Doppler frequency shift. As it is already mentioned, in our study we take into account 28 knot as the maximum average receiver speed to see how this speed affects the maritime channels.

Apparent change in frequency of the i^{th} propagation path due to the motion of the transmitter and/or receiver is named as Doppler effect and it is given by [14]:

$$\Delta f_i = f_0 \left[\frac{d_i V_T}{c} + \frac{a_i V_R}{c} \right] \tag{4.3}$$

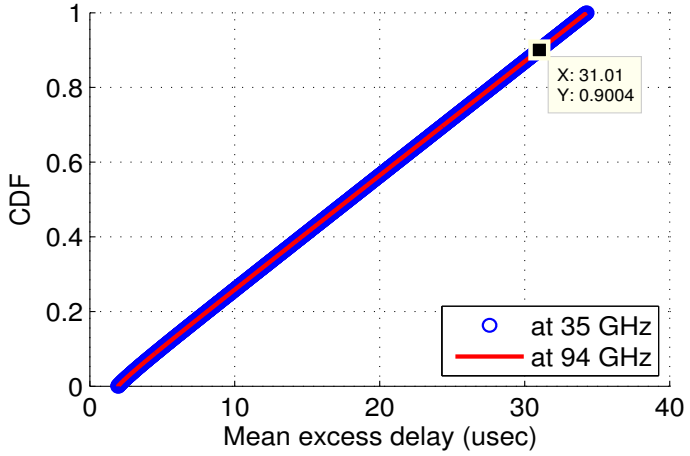

(a)

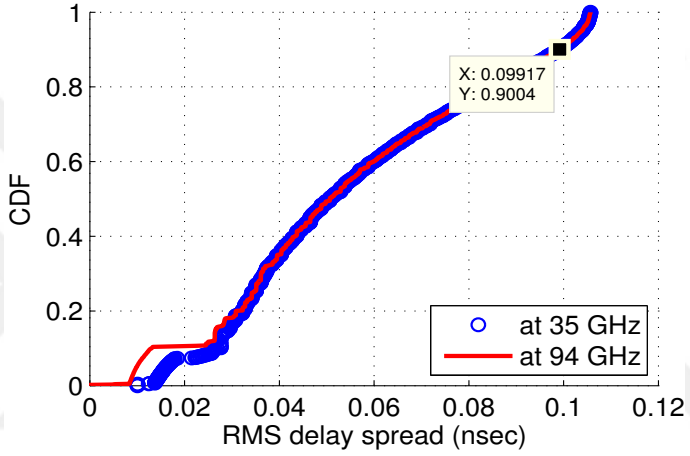

(b)

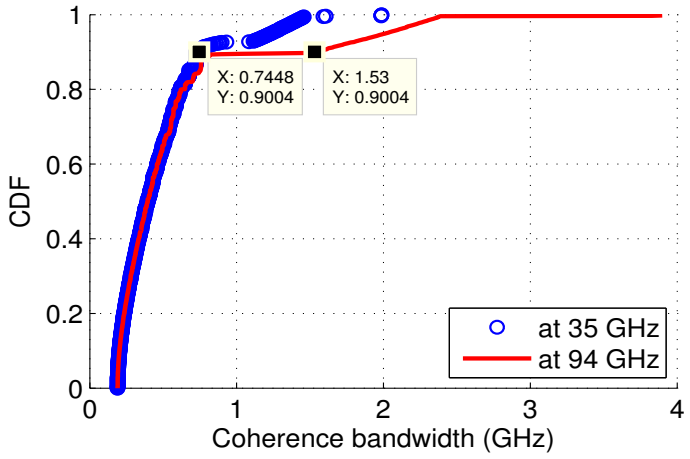

(c)

FIGURE 4.3: CDFs at different frequencies; (a) mean delay, (b) RMS delay spread, and (c) 90% coherence bandwidth.

where V_R and V_T are the velocities of the receiver and transmitter, respectively. a_i and d_i are the directions of arrival and departure of the i^{th} ray, f_0 is the carrier frequency

and c is the speed of light defined as 3×10^8 m/s. Under our assumptions, since the transmitter is fixed at its location, V_T is zero, therefore the equation of Δf_i reduces to

$$\Delta f_i = \frac{a_i V_R}{\lambda} \tag{4.4}$$

where λ is the wavelength of the transmitted signal in meter.

Figure 4.4 demonstrates the Doppler spectrum at 682 sec for both 35 GHz and 94 GHz. By looking at the Doppler spectrum at 682 sec, we observe that the direct path is at -1.6765 kHz with level -112.165 dBm at 35 GHz carrier frequency and -4.5025 kHz with level -120.874 dBm at 94 GHz due to the speed of the vessel. Also, we can observe some further distinct components caused by reflection from the sea surface and diffraction. As the order of diffraction increases, the power of corresponding path will be decreased. For observing how the Doppler spread is affecting the channel within the total receiver route, we have shown the received power versus the Doppler frequency for LoS paths received at all locations. Figure 4.5 illustrates that at the starting point, where the receiver is directly looking at the transmitter, the received power is maximum while the Doppler frequency is minimum. When the receiver is moving far away from the transmitter, the received power decreases and the absolute value of Doppler frequency increases. It should be noted that the maximum absolute value of Doppler frequency obtained through our framework is in a good agreement with the theoretical values, i.e., -1.6805 kHz and -4.5134 kHz maximum Doppler shift at 35 GHz and 94 GHz, respectively. As a result, since the baseband signal bandwidth is much greater than the absolute value of maximum Doppler frequency, the effect of Doppler spread is negligible at the receiver [38]. In the time domain, the coherence time (T_c) related to Doppler spread is actually a measure of time duration over which the channel impulse response is essentially invariant. When the time correlation of the impulse response is 50%, the coherence time is given as [38]

$$T_c = \frac{9}{16\pi f_m} \tag{4.5}$$

The corresponding coherence times at 35 GHz and 94 GHz are approximately 0.1 msec and 0.04 msec, respectively. Therefore, for a digital transmission system with symbol rates larger than $1/T_C$, the channel will effectively not cause distortion due to the motion.

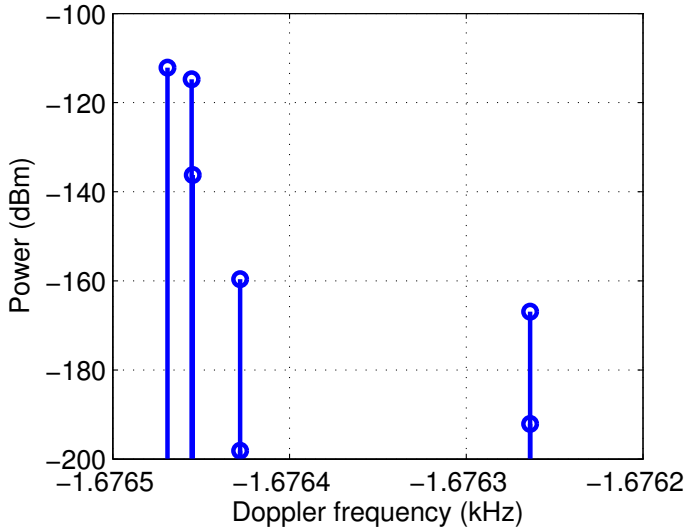

(a)

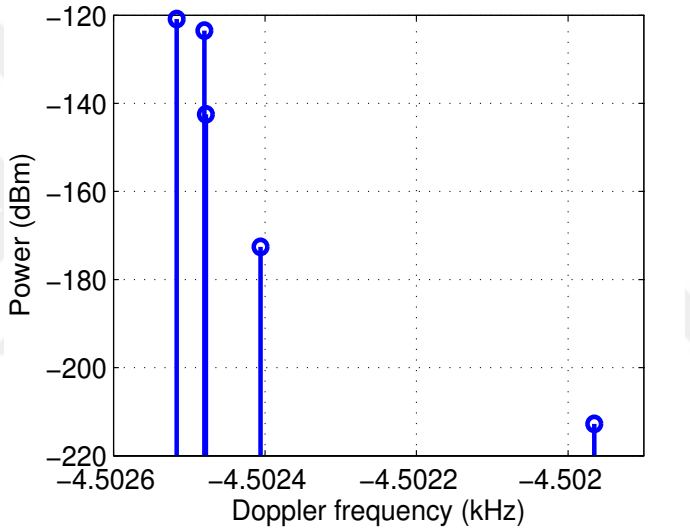

(b)

FIGURE 4.4: Doppler spectrum at 682 sec; (a) at 35 GHz, and (b) at 94 GH.

4.2.3 Coherence Distance

Coherence distance is another important small scale characteristic that can be extracted from the angle of arrival. Coherence distance, D_c, is the amount of separation in space over which a fading channel appears to be unchanged. Based on the value of D_c, we determine the antenna distance for multiple transmit and receive chains that can be used for Multiple Input Multiple Output (MIMO) systems. In this regard, [38] presents an expression to reveal the effect of shape factors (i.e. angular spread (Λ), angular constriction (γ), and azimuth direction of maximum fading (θ_{max})) on D_c. This relation

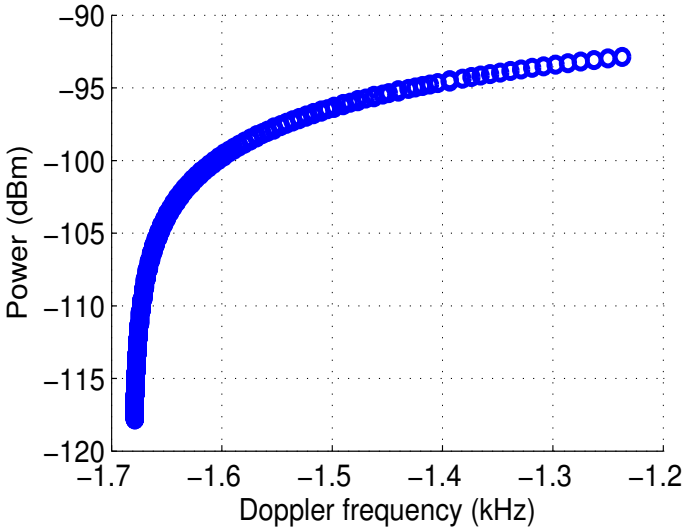

(a)

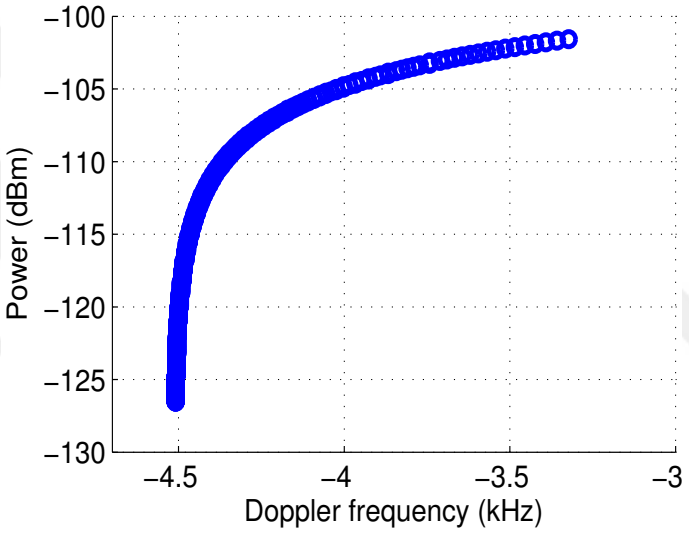

(b)

FIGURE 4.5: Doppler spectrum for the total rout; (a) at 35 GHz, and (b) at 94 GHz.

is given as

$$D_c \approx \frac{\lambda\sqrt{ln2}}{\Lambda\sqrt{23(1-\gamma cos\,[2(\theta-\theta_{max})])}} \tag{4.6}$$

where λ is the wavelength and θ is the direction of arrival. Based on the simulation outcomes, all received paths are coming almost from the same direction at both 35 GHz and 94 GHz. In fact, the results indicate that Λ is about zero and therefore D_c is a very large value. In another words, since the coherence distance is so large and Λ is too small, there is no space diversity over the sea surface under our assumed scenario [39].

4.3 Chapter Conclusions

In this chapter, the small scale variations of LoS maritime channel have been investigated at two different frequencies bands, i.e., 35 GHz and 94 GHz. In particular, the CDF were computed for mean excess delay, RMS delay spread, 90% coherence bandwidth and coherence time at all receiver locations up to 10 km. According to the CDF results, the maritime channel can be regarded as frequency non-selective over a bandwidth of 744 MHz and 1.53 GHz at 35 GHz and 94 GHz, respectively, which is large enough to have high data rate transmission and support the data rate requirements of 5G systems. Additionally, the Doppler spectrum was computed to show that the channel under investigation is unaffected by the frequency shift due to the vessel movements. Therefore, the effect of Doppler frequency is negligible for the sea channel. Also, the corresponding coherence times are in the order of msec which are long enough not to cause distortions due to the motion. Accordingly, for maritime environment, it would be possible to apply simple communication systems, which are operating at 35 GHz and 94 GHz. Finally, this study shows that MIMO is not suitable for the simulated scenarios since there is no space diversity for off shore ship to ship sea channels.

Chapter 5

Conclusions and Future Works

In this thesis study, an investigation of maritime LoS millimeter radiowave propagation was presented at two frequencies, 35 GHz and 94 GHz. We discussed the effect of distance between transmitter and receiver on the propagation loss, received power, and RMS delay spread. Our results demonstrate that although there is a good agreement between simulated results and analytical models (i.e. 2-ray and FSL) for lower frequencies, for the interested millimeter radiowave frequencies to this study (i.e., 35 GHz and 94 GHz), both FSL and 2-ray models are not able to model the channel over the sea surface. It is observed that for short ranges, almost less than 4 km, prediction of 2-ray model is still reliable, while FSL model could only predict the exponentially increasing of propagation loss without following the exact path loss trend even for short ranges. Our results also demonstrate that in order to have more realistic channel model, we need consider the effect of ray spacing, Earth's curvature, and sea surface roughness in our simulations and modeling approach.

Furthermore, the small scale variations of LoS maritime channel were investigated at 35 GHz and 94 GHz. In particular, the CDF were computed for mean excess delay, RMS delay spread, 90% coherence bandwidth and coherence time at all receiver locations up to 10 km. According to the CDF results, the maritime channel can be regarded as frequency non-selective over a bandwidth of 744 MHz and 1.53 GHz at 35 GHz and 94 GHz, respectively, which is large enough to have high data rate transmission and support the data rate requirements of 5G systems. Additionally, the Doppler spectrum was computed to show that the channel under investigation is unaffected by the frequency

shift due to the vessel movements. Therefore, the effect of Doppler frequency is negligible for the sea channel. Also, the corresponding coherence times are in the order of msec which are long enough not to cause distortions due to the motion. Accordingly, for maritime environment, it would be possible to apply simple communication systems, which are operating at 35 GHz and 94 GHz. Finally, this study shows that MIMO is not suitable for the simulated scenarios since there is no space diversity for off shore ship to ship sea channels.

As our future work, we are going to obtain a comprehensive equation that considers the effective parameters on marine channel such as Earth's curvature and sea surface reflection coefficient, all together. In addition, we want to focus on a related measurement campaign to study more on both off shore and on shore scenarios. Moreover, we will take into consideration the effect of 3rd party ships in order to model the reflection of millimeter waves from the other objects rather than the sea surface.

Bibliography

[1] V. S. Jain, S. Jain, L. Kurup, and A. Gawade. Overview on Generations of Network: 1G, 2G, 3G, 4G, 5G. *IOSR Journal of Electronics and Communication Engineering*, 9(3), 2014.

[2] What are the hot topics in research for 5G? `https://behindthesciences.com/towards-5g/what-are-the-hot-topics-in-research-for-5g/`, 2017.

[3] What is 5G? 5G vs 4G and the future of mobile networks. `http://gearopen.com/techbuzz/what-is-5g-5g-vs-4g-and-the-uture-of-mobile-networks-23361/`, 2017.

[4] P. Sharma. Evolution of mobile wireless communication networks-1G to 5G as well as future prospective of next generation communication network. *International Journal of Computer Science and Mobile Computing*, 2(8):47–53, 2013.

[5] J. Zh. Sun, J. Sauvola, and D. Howie. Features in future: 4G visions from a technical perspective. In *Global Telecommunications Conference, 2001. GLOBECOM'01. IEEE*, volume 6, pages 3533–3537. IEEE, 2001.

[6] Ms A. Gawas. An Overview on Evolution of Mobile Wireless Communication Networks: 1G-6G. *International Journal on Recent and Innovation Trends in Computing and Communication*, 3(5):3130–3133, 2015.

[7] X. Li, A. Gani, R. Salleh, and O. Zakaria. The future of mobile wireless communication networks. In *Communication Software and Networks, 2009. ICCSN'09. International Conference on*, pages 554–557. IEEE, 2009.

[8] Sh. Jaiswal, A. Kumar, and N. Kumari. Development of Wireless Communication Networks: From 1G to 5G. *International Journal Of Engineering And Computer Science*, 3(5):6053–6056, 2014.

[9] T. Wang, G. Li, B. Huang, Q. Miao, J. Fang, P. Li, H. Tan, W. Li, J. Ding, J. Li, et al. Spectrum Analysis and Regulations for 5G. In *5G Mobile Communications*, pages 27–50. Springer, 2017.

[10] Th. S Rappaport, G. R MacCartney, M. K Samimi, and S. Sun. Wideband millimeter-wave propagation measurements and channel models for future wireless communication system design. *IEEE Transactions on Communications*, 63(9):3029–3056, 2015.

[11] K. D. Anderson. 94-GHz propagation in the evaporation duct. *IEEE transactions on antennas and propagation*, 38(5):746–753, 1990.

[12] A. Danklmayer, G. Biegel, T. Brehm, S. Sieger, and J. Förster. Millimeter wave propagation above the sea surface during the squirrel campaign. In *Radar Symposium (IRS), 2015 16th International*, pages 300–304. IEEE, 2015.

[13] H. H. Fuchs. Microwave and millimeterwave propagation within the marine boundary layer. *German Microwave Conference*, 2006.

[14] Remcome, Wireless InSite 2.6.3. `http://www.remcom.com/wireless-insite`, 2016.

[15] J. C. Reyes-Guerrero, G. Sisul, and L. A Mariscal. Measuring and estimating the propagation path loss and shadowing effects for marine wireless sensor networks at 5.8 GHz. In *Telecommunications Forum (TELFOR), 2012 20th*, pages 323–226. IEEE, 2012.

[16] J. C. Reyes-Guerrero and L. A. Mariscal. Experimental time dispersion parameters of wireless channels over sea at 5.8 GHz. In *ELMAR, 2012 Proceedings*, pages 89–92. IEEE, 2012.

[17] M. S. Choi, S. Park, Y. Lee, and S. R. Lee. Ship to Ship Maritime Communication for e-Navigation Using WiMAX. *International Journal of Multimedia and Ubiquitous Engineering*, 9(4):171–178, 2014.

[18] JC. Reyes-Guerrero, M. Bruno, L. A Mariscal, and A. Medouri. Buoy-to-ship experimental measurements over sea at 5.8 GHz near urban environments. In *Mediterranean Microwave Symposium (MMS), 2011 11th*, pages 320–324. IEEE, 2011.

[19] Y. H. Lee, F. Dong, and Y. S. Meng. Near sea-surface mobile radiowave propagation at 5 GHz: measurements and modeling. *Radioengineering*, 2014.

[20] Y. S. Meng and Y. H. Lee. Measurements and characterizations of air-to-ground channel over sea surface at C-band with low airborne altitudes. *IEEE Transactions on Vehicular Technology*, 60(4):1943–1948, 2011.

[21] A. Coker, L. Straatemeier, T. Rogers, P. Valdez, D. Cooksey, and K. Griendling. Maritime channel modeling and simulation for efficient wideband communications between autonomous unmanned surface vehicles. In *Oceans-San Diego, 2013*, pages 1–9. IEEE, 2013.

[22] J.C. Reyes-Guerrero and L.A. Mariscal. 5.8 GHz propagation of low-height wireless links in sea port scenario. *Electronics Letters*, 50(9):710–712, 2014.

[23] X. Zhao, S. Huang, and H. Fan. Influence of sea surface roughness on the electromagnetic wave propagation in the duct environment. In *Geoscience and Remote Sensing (IITA-GRS), 2010 Second IITA International Conference on*, volume 1, pages 467–470. IEEE, 2010.

[24] K. Maliatsos, P. Loulis, M. Chronopoulos, Ph. Constantinou, P. Dallas, and M. Ikonomou. Measurements and wideband channel characterization for over-the-sea propagation. In *Wireless and Mobile Computing, Networking and Communications, 2006.(WiMob'2006). IEEE International Conference on*, pages 237–244. IEEE, 2006.

[25] Y. H. Lee, F. Dong, and Y. S. Meng. Stand-off distances for non-line-of-sight maritime mobile applications in 5 GHz band. *Progress In Electromagnetics Research B*, 54:321–336, 2013.

[26] F. Dong and Y. H. Lee. Non-line-of-sight communication links over sea surface at 5.5 GHz. In *Microwave Conference Proceedings (APMC), 2011 Asia-Pacific*, pages 1682–1685. IEEE, 2011.

[27] X. Cao and T. Jiang. Research on sea surface ka-band stochastic multipath channel modeling. In *Antennas and Propagation (APCAP), 2014 3rd Asia-Pacific Conference on*, pages 675–678. IEEE, 2014.

[28] K. Yang, T. Roste, F. Bekkadal, and T. Ekman. Land-to-Ship Radio Channel Measurements over Sea at 2 GHz. In *2010 6th International Conference on Wireless Communications Networking and Mobile Computing (WiCOM)*, pages 1–4, Sept 2010. doi: 10.1109/WICOM.2010.5600916.

[29] K. Yang, T. Roste, F. Bekkadal, and T. Ekman. Experimental multipath delay profile of mobile radio channels over sea at 2 GHz. In *Antennas and Propagation Conference (LAPC), 2012 Loughborough*, pages 1–4. IEEE, 2012.

[30] J. C. Reyes-Guerrero. Experimental Broadband Channel Characterization in a Sea Port Environment at 5.8 GHz. *IEEE Journal of Oceanic Engineering*, 41(3):509–514, 2016.

[31] W. C. Lee. *Mobile communications engineering*. McGraw-Hill Professional, 1982.

[32] H. V. Hitney and L. R. Hitney. Frequency diversity effects of evaporation duct propagation. *IEEE Transactions on Antennas and Propagation*, 38(10):1694–1700, 1990.

[33] Pierson- Moskowitz Sea Spectrum. `http://www.syqwestinc.com/media/support/performance-prediction.pdf`, 2016.

[34] N. Mehrnia and M. K. Özdemir. Novel maritime channel models for millimeter radiowaves. In *Software, Telecommunications and Computer Networks (SoftCOM), 2016 24th International Conference on*, pages 1–6. IEEE, 2016.

[35] M. Landrø, L. Amundsen, and J. Langhammer. Repeatability issues of high-frequency signals emitted by air-gun arrays. *Geophysics*, 78(6):P19–P27, 2013.

[36] What is the average speed of a ship? `http://www.quora.com/Merchant-Navy-What-is-the-average-speed-of-a-ship`, 2016.

[37] Cruise Ship/Cruising Speed. `http://www.cruisemapper.com/wiki/762-fastest-cruise-ship-speed`, 2016.

[38] Th. S. Rappaport et al. *Wireless communications: principles and practice*, volume 2. Prentice Hall PTR New Jersey, 1996.

[39] N. Mehrnia and M. K. Özdemir. Multipath delay profile and doppler spread of millimeter radiowaves over the sea channel. In *Black Sea Conference on Communications and Networking (BlackSeaCom), 2017 International Conference on*, pages 1–5. IEEE, 2017.